**Indonesian Review of Physics (IRiP)**
Vol.7, No.1, June 2024, pp. 1 - 22

p-ISSN: 2621-3761 | e-ISSN: 2621-2889
DOI: 10.12928/irip.v7i1.9562

# Implantable Antennas for Biomedical Purposes: State-of-the-Art, Challenges, and Future Directions

**Muhammad Miftahul Amri[1]*, Urfa Khairatun Hisan[2], Dwi Sulisworo[3]**
[1] Department of Electrical Engineering, Faculty of Industrial Technology, Universitas Ahmad Dahlan, Indonesia
[2] Medicine Study Program, Faculty of Medicine, Universitas Ahmad Dahlan, Indonesia
[3] Doctoral Program of Education, Faculty of Teacher Training and Education, Universitas Ahmad Dahlan, Indonesia
Email: muhammad.amri@te.uad.ac.id*

**Article Info**

**Article History**
Received: Dec 23, 2023
Revision: Apr 24, 2024
Accepted: May 28, 2024

**Keywords:**
Implantable Antennas
Implantable Medical Devices
Biomedical Engineering
Rectifier Antenna (Rectenna)
Biocompatibility
Antenna Design
Miniaturized Antenna

**ABSTRACT**

This article provides a comprehensive review of implantable antennas in the context of their application within the biomedical field. Through a systematic exploration of cutting-edge developments and associated challenges, a thorough understanding of antenna design, performance considerations, and safety implications is obtained. The investigation thoroughly examines diverse antenna types, including planar, microstrip, fractal-geometry, and others, elucidating the design considerations that govern their suitability for a wide array of implantable medical devices (IMDs). Substrate and material choices are critical factors influencing antenna efficiency and biocompatibility. The utilization of available frequency bands is evaluated, highlighting the inherent tradeoffs that dictate their applicability in biomedical applications. Additionally, the promising domain of rectenna technology is explored for its potential in sustainable energy harvesting. The discourse on miniaturization techniques underscores their pivotal role in enabling the seamless integration of antennas within intricate implant structures. Safety aspects are paramount, encompassing metrics such as specific absorption range (SAR), maximum permissible exposure (MPE) limits, and thresholds for localized temperature changes. The intricate interplay between human body effects and antenna performance is briefly elaborated. Methodologies for thorough evaluation, spanning computer simulations, as well as experiments in in vivo and in vitro scenarios, are discussed for their pivotal role in iteratively refining antenna functionality.



To cite this article:
M. M. Amri, U. K. Hisan, and D. Sulisworo, "Implantable Antennas for Biomedical Purposes: State-of-the-Art, Challenges, and Future Directions," *Indones. Rev. Phys.*, vol. 7, no. 1, pp. 1–22, 2024, doi: 10.12928/irip.v7i1.9562

## I. Introduction

In recent years, there has been a growing interest in the development of implantable antennas for biomedical purposes. Implantable antennas offer the potential to enable wireless communication and power transfer within the human body, facilitating a wide range of applications in healthcare and biomedicine [1]. These antennas can serve as vital components in implantable devices for monitoring physiological parameters, delivering therapeutic interventions, and establishing seamless communication with external devices (see Fig. 1).

The increasing demand for miniaturized and wireless biomedical devices has driven the evolution of implantable antenna technology. Traditional wired systems often pose limitations in terms of invasiveness, mobility, and patient convenience [2]. Implantable antennas provide a wireless solution, eliminating the need for cumbersome wires and enhancing patient mobility and comfort [3].

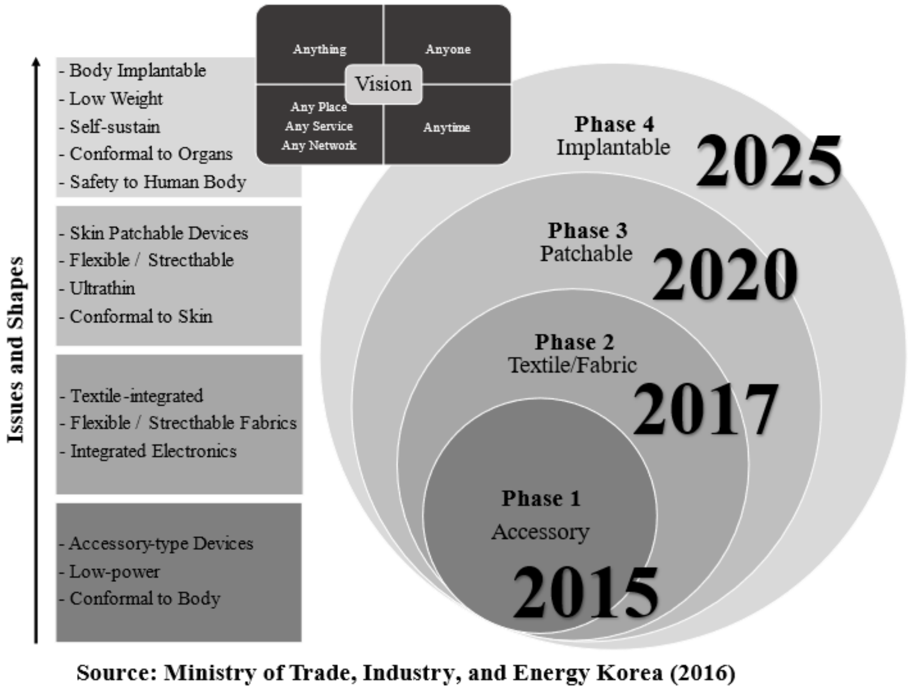


**Figure 1.** Directions and roadmap for implantable devices, made by Korean Ministry of Trade, Industry, and Energy (2016) [4].

One of the key challenges in the design of implantable antennas is their integration within the human body. The human body consists of various tissues and fluids, each with different dielectric properties and absorption characteristics at different frequencies. These factors pose significant design considerations for implantable antennas to ensure efficient and reliable wireless communication and power transfer.

In addition to integration challenges, implantable antennas must adhere to strict size constraints. Miniaturization is essential to accommodate implantation in small anatomical spaces and to minimize the impact on the surrounding tissues. However, reducing antenna size while maintaining adequate performance and bandwidth remains a significant design challenge. Another critical aspect in the development of implantable antennas is their biocompatibility. Since the antenna is in direct contact with body tissues and fluids, it is crucial to ensure that the materials used are biocompatible and do not cause adverse reactions or tissue damage. The choice of materials and fabrication techniques becomes critical in achieving biocompatibility while maintaining antenna performance.

Moreover, implantable antennas must address power consumption and efficiency concerns. Many implantable devices are powered by external sources or harvest energy from the surrounding environment. Efficient wireless power transfer (WPT) and energy harvesting techniques are essential to prolong the lifespan of implantable devices and reduce the need for frequent battery replacements or invasive procedures for recharging.

The state-of-the-art research in implantable antennas for biomedical purposes has witnessed significant progress. Researchers have explored various antenna designs, including patch antennas, helical antennas, and meandered antennas, to address the challenges of size, biocompatibility, and performance. Furthermore, advancements in simulation tools, fabrication techniques, and wireless communication protocols have contributed to the continuous improvement of implantable antenna systems.

Implantable devices, or at least the idea of implantable devices, have existed since decades ago. In the last couple of years, the number of devices implanted in human beings has risen significantly. In Figure 1, we present the directions and roadmap for implantable devices published by the Korean Ministry of Trade, Industry, and Energy (2016) [4].

There are various reasons for someone to implant electronic devices in their body. Ranging from biomedical applications (e.g., implantable pacemaker [5], brain implant [6], intracranial pressure and temperature sensor [7], cochlear implant [8], in vivo dosimeter [9], retinal implant [10], etc.), which are the most common applications, implanted radiofrequency identification (RFID) for personal identifications and daily functions [11], to research and communication purposes (muscle [12] and brain activity sensors [13]).

Illustrated in Figure 2, in order for the implantable devices to function properly, many devices are equipped with antennas to communicate with out-body devices. Due to this particular reason, numerous researchers have tried to propose implantable antenna designs. Aside from the obvious constraint (i.e., small sizes and safe-for-human

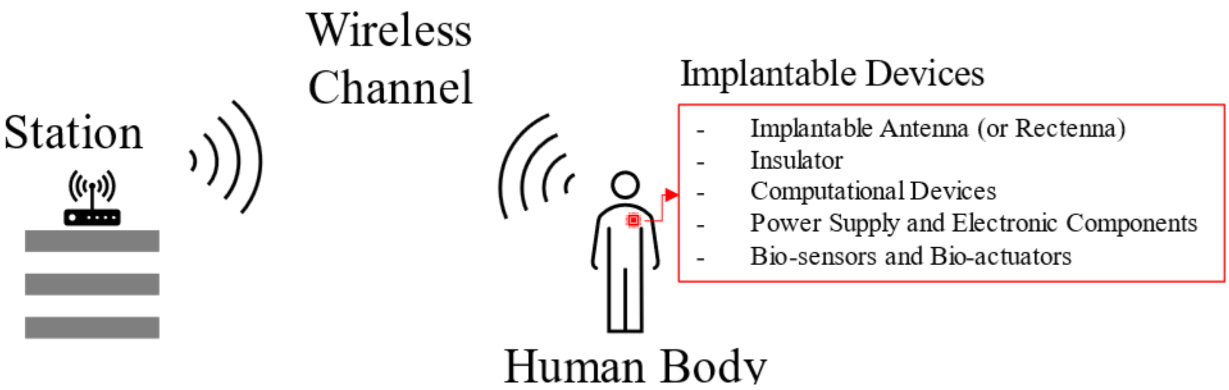


**Figure 2.** Wireless implantable systems for data telemetry and power transfer.

body), several factors need to be considered in designing an implantable antenna.

As aforementioned, designing an implantable antenna is, arguably, more complex than designing an antenna for conventional applications. In implantable antenna design, one must optimize the antenna performance (e.g., gain, bandwidth, directivity, etc.), while still satisfying the dimension and safety constraint. Nevertheless, the development of implantable antennas for biomedical purposes offers promising opportunities for revolutionizing healthcare and biomedicine. This review article aims to comprehensively examine state-of-the-art implantable antennas for biomedical purposes. By analyzing design principles, fabrication techniques, challenges, and future directions, this article seeks to provide a nuanced understanding of the critical role implantable antennas play in telemetry-enabled implanted medical devices (IMDs). Drawing insights from interdisciplinary fields, this review intends to serve as a valuable resource for researchers, engineers, and healthcare professionals, fostering advancements in implantable antenna technology and its integration into the evolving landscape of wireless-enabled medical solutions. By understanding the existing knowledge and research gaps, further advancements can be made toward the development of efficient and reliable implantable antenna systems for improved healthcare outcomes. The contributions of this article are threefold:

- We summarized the state-of-the-art and recent developments of implantable antennas, particularly for IMDs and biomedical applications. The findings were derived from more than 100 selected high-quality published literature on implantable antennas and IMDs.
- We comprehensively discussed the challenges and difficulties in implantable antenna design for biomedical purposes.
- We briefly present a discussion on the opportunities, path ahead, and future directions of implantable antennas for biomedical applications.

## II. Material and Methods

As aforementioned, in this article, we aim to summarize the state-of-the-art implantable antennas, particularly for biomedical purposes. Further, this article also discusses the recent developments, challenges, and future directions for implantable antennas for biomedical applications. The findings were synthesized from hundreds of articles that were published in the last couple of decades. All of the collected articles were written in English and were gathered from major publishers such as IEEE, Scopus, Springer, MDPI, ACM, and Nature.

The rest of this article is organized as follows. In Section 3, we present our findings, followed by a brief critical discussion derived from the findings. In this section, we first presented various IMD applications and how IMD could benefit from the presence of an implantable antenna. Then, we present our findings on the implantable antenna design, consisting of various antenna types as well as a diverse range of antenna material selections. In the third subsection, we briefly discuss the available frequency bands for biomedical purposes, particularly for implantable antenna applications, along with the advantages and disadvantages. As an extended function of the implantable antenna, WPT and rectifier antenna (rectenna) are discussed in subsection four. Then, in the fifth and six subsections, respectively, we present the antenna miniaturization technique, followed by the discussion on antenna biocompatibility and user safety. Human body effects on implantable antenna characteristics and performances are discussed in the penultimate subsection of Section 3. In the last subsection of Section 3, we present various methods to test the implantable antenna, ranging from computer simulations and experiments on human phantoms to experiments conducted on living organisms. Finally, we concluded the findings of this study in Section 4.

## III. Results and Discussion

### IMDs and Implantable Antenna Applications

**Table 1.** Various Implantable Medical Devices (IMDs) Applications

| IMD Type | IMD Functions | Functions of the Antenna |
| --- | --- | --- |
| Implantable Pacemaker | Regulates and controls the heart's rhythm by emitting electrical impulses. | Data telemetry, wireless power transfer (WPT) |
| Implantable Cardioverter-Defibrilator | Monitors and corrects irregular heartbeats by delivering controlled electrical shocks. | Data telemetry |
| Neural Implants | Interface with the nervous system to restore sensory or motor functions impaired by neural disorders. | Data telemetry |
| Muscle Biosensor | Measures muscle activity and movement patterns. | Data telemetry |
| Retinal Implants | Stimulate the retina's cells to restore partial vision in individuals with retinal degeneration. | Data telemetry |
| Cochlear Implants | Provide auditory sensations by directly stimulating the auditory nerve in the inner ear. | Data telemetry |
| Glucose Biosensor | Monitors blood glucose levels for diabetes management through continuous sensing. | Data telemetry, sensor |
| Implantable Loop Recorder | Records and monitors the heart's electrical activity to diagnose arrhythmias. | Data telemetry |
| Deep Brain Stimulators | Deliver controlled electrical stimulation to specific brain regions for treating neurological disorders. | Data telemetry |
| Implanted Drug delivery | Administers precise doses of medication directly to targeted areas, enhancing therapeutic effectiveness and minimizing side effects. | Data telemetry, control |
| Implanted Temperature Sensor | Measures internal body temperature for various medical applications, including fever detection and monitoring during surgeries. | Data telemetry, sensor |
| Implanted RFID | Personal identification. | Data telemetry, sensor |
| Implanted Oximeter | Measures oxygen saturation in body tissues, aiding in monitoring respiratory and cardiovascular health. | Data telemetry, sensor |
| Implantable Brain-Machine Interface | Allows direct communication between the brain and external devices, enabling control or communication through neural signals. | Data telemetry |

Thanks to the rapid developments of biomedical engineering research and its supporting technologies, IMDs have witnessed major advancement in the past few decades. To this date, many IMD developments have reached the mature stages and have been deployed in actual human users. However, not all IMDs are equipped with electronic devices. In fact, prostheses, intraocular lenses, and tooth implants are three of the most common IMDs, all of which are usually not equipped with electronic components. As summarized in Table 1, in this work, we would like to focus only on electronic-equipped IMDs that could benefit from implantable antennas.

## Implantable Antenna Design

Similar to conventional antennas, there are various design topologies for implantable antennas. This subsection discusses some of the most common topologies for implantable antenna design.

In Table 2, we gathered some studies on implantable antenna designs. As observed, various design topologies, as well as a diverse selection of materials, have been proposed for implantable antenna designs. The proposed antennas operate at different frequency bands, such as 0.402 GHz, 0.915 GHz, 1.45 GHz, 2.4 GHz, and 4.8 GHz. As in Table 2, diverse antenna dimensions, as well as performances (e.g., gain and bandwidth), have been observed. The antenna bandwidth ($BW$) can be expressed as

$$BW = 100 \times \left(\frac{F_H - F_L}{F_C}\right), \quad (1)$$

where $F_H$ is the upper frequency bound, $F_L$ is the lower frequency bound, and $F_C$ is the center frequency. Antenna bandwidth is usually quoted in terms of voltage standing wave ratio (VSWR), that is

$$VSWR = \frac{1+|\Gamma|}{1-|\Gamma|}, \quad (2)$$

where $\Gamma$ is the antenna reflection coefficient, expressed as $\frac{\vartheta^2 - \vartheta^1}{\vartheta^2 + \vartheta^1}$, where $\vartheta = \sqrt{\left(\frac{j\omega\mu}{\sigma + j\omega\epsilon_r}\right)}$ is the intrinsic impedance [14]. Then, $\omega$ (rad/m), $\mu$ (H/m), and $\epsilon_r$, respectively, are the angular frequency of the propagation media (i.e., human tissue), permeability of the propagation media (i.e.,


p-ISSN: 2621-3761
e-ISSN: 2621-2889

human tissue), and antenna permittivity. The antenna gain ($G_A$) can be expressed as [15]

$$G_A(dB) \;=\; 10\;log10\left(\frac{4\pi\eta A}{\lambda^2}\right). \qquad (3)$$

In (3), $\eta = \frac{\text{Radiated Power}}{\text{Source Power}}$, is the radiation efficiency [1]. $A$ denotes the antenna's physical aperture, and $\lambda$ is the radio frequency wavelength. Note that the gain of implantable antennas is usually negative. This is due to the lossy nature of human body parts.

**Table 2.** Recent Studies on Implantable Antennas

| Ref. | Year | Topology | Frequency (GHz) | Gain (dBi) | Dimension (mm³) | Bandwidth (%) | Material |
|---|---|---|---|---|---|---|---|
| [16] | 2018 | Slotless and vialess patch | 0.915, 2.45 | -28.5, -22.8 | 8 × 6 × 0.5 | 9.84, 8.57 | Rogers RO6010 |
| [17] | 2021 | Adhesive planar antenna | 2.4, 3.2, 4.8 | -8, -5, -9 | 24 × 24 × 0.787 | 42, 1.2, 80 | Duroid RT5880 |
| [18] | 2019 | Spiral planar antenna | 0.402 | n/a | 5 × 5 × 0.89 | n/a | Rogers RO3210 (substrate), RO3006 (superstrate) |
| [19] | 2018 | Meander structure with slot and fractal geometry | 2.45 | n/a | 11.44 × 11.44 × 0.275 | 1.5 | Silicon Substrate ($\epsilon_r = 11.7$) |
| [20] | 2018 | Conformal circular polarization (CP) patch | 2.45 | -29.1 | 14.2 × 16.64 × 0.254 | 31 | Rogers RO6010 |
| [21] | 2018 | CP patch | 0.915 | -32.8 | $\pi$ × 4.72 × 1.27 | 17.5 | Rogers RO3010 |
| [22] | 2018 | Dual-ring slot | 2.45 | -9 | 10 × 10 × 0.4 | 57 | Kapton polyamide substrate |
| [23] | 2018 | CP antenna | 0.915 | -29 | 11 × 11 × 1.27 | 1.2 | Rogers RO3010 |
| [24] | 2018 | Circular patch | 0.4035, 0.4339, 2.45 | n/a | $\pi$ × 7.52 × 1.92 | 28 (at 0.402-0.4348 GHz), 10 (at 2.45 GHz) | Rogers RO3010 |
| [25] | 2019 | Pin-loaded annular ring (PLAR) CP antenna | 2.45 | -22.7 | $\pi$ × 52 × 1.27 | 12.4 | Rogers RO3010 |
| [26] | 2019 | Loop | 0.92, 2.45 | -29.33, -21 | 10 × 10 × 0.6 | 12.2, 123 | Rogers RO3010 |
| [27] | 2019 | Flower-shape | 0.928, 2.45 | -28.44, -25.65 | 7 × 7.2 × 0.2 | 19.8, 8.9 | Rogers ULTRALAM 3850HT |
| [28] | 2019 | Planar inverted F-antenna (PIFA) | 0.402 | -34.9 | 23 × 16.4 × 1.27 | 0.13 | Rogers RO6010 |
| [29] | 2019 | Circular patch | 0.402, 2.4 | -33.1, -14.55 | $\pi$ × 102 × 2.54 | 31.6, 37.6 | Rogers RO6010 |
| [30] | 2020 | Meandered, triangular microstrip (intraocular). PIFA (extraocular, 1.45 GHz). Rectangular microstrip (extraocular, 2.45 GHz) | 1.45, 2.45 | -36, -35 | Intraocular = 6.25 × 6 × 0.63 (1.45 GHz), 7 × 6.93 × 0.63 (2.45 GHz). Extraocular = 26 × 24 × 1.43 (1.45 GHz), 28 × 24 × 1.43 (1.45 GHz) | 4.1, 36.7 | Duroid RT6010 |
| [31] | 2022 | Folded meander | 2.4 | -24.9 | 3 × 3 × 0.5 | 22 | Rogers RO3010 |
| [32] | 2022 | Square patch with loop | 2.45 | -16.7 | 8 × 8 × 0.8 | 64.9 | Duroid RT5880 |
| [33] | 2022 | Double-layer patches | 2.4 | -9.7 | 2.6 × 3 × 0.381 | 6.15 | Duroid RT6010 |
| [34] | 2022 | Rectangular patch with coaxial feed | 2.4, 4.8 | -26, -8.8 | 8.5 × 8.5 × 1.27 | 3.33, 3.65 | Rogers RO3010 |
| [35] | 2022 | Three concentric split ring elements | 0.402, 0.433, 1.4, 2.4 | -42.53, -37.24, -23.35, -18.34 | 9 × 9 × 1.27 | 51.2, 51.2, 3.3, 14.9 | Rogers RO3010 |
| [36] | 2022 | PIFA | 0.4025, 2.45 | -31, -22 | 19 × 27 × 0.635 | 7, 9.19 | Rogers RO6010 |
| [37] | 2022 | C-shaped slot | 0.915, 2.4 | -28.9, -29.5 | 7.9 × 7.7 × 1.27 | 44.2, 33.5 | Rogers RO3210 |
| [38] | 2022 | Slotted patch | 0.915 | -28 | 7 × 7 × 0.254 | 21.8 | Duroid RT5880 |


p-ISSN: 2621-3761
e-ISSN: 2621-2889

| | | | | | | | |
|---|---|---|---|---|---|---|---|
| [39] | 2022 | Rectangular patch | 2.4 | -20.71 | 7 × 7 × 0.2 | 35.7 | Rogers ULTRALAM 3850HT |
| [40] | 2023 | Stacked parasitic structure | 2.4 | -24.7 | 9.8 × 9.8 × 0.889 | 30 | Rogers RO6010 |
| [41] | 2023 | Slotted rectangular patch with slot and truncated little patch | 2.45 | -15.8 | 21 × 13.5 × 0.254 | 47.7 | Duroid RT5880 |
| [42] | 2023 | Meandered radiator patch | 2.29 | -26 | 5 × 5 × 0.26 | 29 | Rogers RO3003 |
| [43] | 2023 | Meander-line | 1.4, 2.4 | -37.7, -21 | 10 × 10 × 0.635 | 3.57, 6.37 | Duroid RT6010 |
| [44] | 2023 | Gosper curve fractal-based geometry PIFA | 0.402 | -39.58 | $\pi$ × 52 × 0.762 | 10.1 | Rogers RO3010 |
| [45] | 2023 | Conceived antenna | 0.915, 2.45 | -28.3, -18.5 | 7 × 7 × 0.2 | 18.03, 25.51 | Flexible biocompatible polyamide material ($\epsilon_r = 4.2, \tan\delta = 0.002$) |
| [46] | 2023 | Inverted L-C antenna | 0.4025, 2.45, 2.95 | -46, -33.55, -41.4 | 20 × 12 × 2.2 | 3.5, 12.2, 21.0 | Rogers RO3010 |
| [47] | 2023 | Four-port MIMO antenna | 2.45 | -20.1 | 6.2 × 5.2 × 0.127 | 14.2 | Rogers RO3010 |
| [48] | 2019 | Spiral-shaped antenna | 0.402, 0.433, 1.6, 2.45 | -30.5, -30, -22.6, -18.2 | 7 × 6.5 × 0.377 | 100 | Rogers RO6010 |
| [49] | 2023 | Two-arm rectangular spiral microstrip antenna | 2.45 | -18.41 | 10 × 10 × 2.56 | 4.89 | Rogers RO3210 |

Implantable rectenna for WPT applications.
Implantable antenna for simultaneous wireless information and power transfer (SWIPT) applications.

## Antenna Type

### A. Plannar Antennas

Planar antennas are among the antenna topologies that are most used worldwide for conventional antenna design. Similar to the conventional antenna, planar antennas are also commonly used in implantable antenna design. In [17], the authors proposed an implantable planar antenna operating at a tri-band frequency (i.e., 2.4, 3.2, 4.8 GHz). This antenna was fabricated on a Duroid RT5880 flexible substrate with 24 × 24 × 0.787 mm3 dimensions. Figure 3 presents the overall design of the proposed antenna. The proposed antenna managed to achieve peak gains of at least -8, -5, and -9 dBi. In [18], a 0.402 GHz spiral-shaped planar antenna was proposed. In this work, a Rogers RO3210 was used as a substrate material, and a Rogers RO3006 was used as a superstrate material (See Figure 4). The dimensions of the antenna were 5 × 5 × 0.89 $mm^3$. In [46], an inverted L-C implantable planar antenna was proposed. This antenna worked at 0.4025, 2.45, and 2.95 GHz frequency bands. The dimensions were 20 × 12 × 2.2. The peak gains and bandwidths for 0.4025, 2.45, and 2.95 GHz frequency were, respectively, -46 dBi, -33.55 dBi, -41.4 dBi, and 3.5%, 12.2%, 21.0%.

### B. Microstrip Antennas

Meandered triangular microstrip implantable antennas have been proposed as intraocular elements for the implanted and external subsystems of a wireless retinal

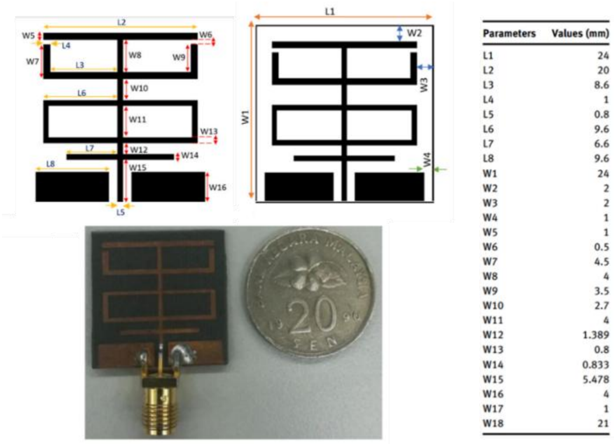


**Figure 3.** Implantable adhesive planar antenna proposed in [17].

prosthesis in [30]. The proposed antennas were designed to work at 1.45 GHz and 2.45 GHz. The measured gain of the system was -36 dBi and -35 dBi, respectively, at 1.45 GHz and 2.45 GHz. The proposed antennas were fabricated on an RT6010 substrate. The proposed system achieved a relatively wide bandwidth of 4.1% at 1.45 GHz and 36.7% at 2.45 GHz. The structures of the proposed antennas are depicted in Figure 5. Another microstrip


p-ISSN: 2621-3761
e-ISSN: 2621-2889

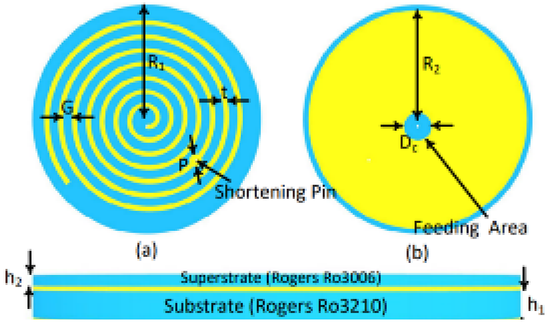


| Parameters | Dimensions (mm) |
|---|---|
| $R_1$ | 5 |
| $R_2$ | 4.75 |
| $D_c$ | 1.2 |
| t | 0.2 |
| G | 0.3 |
| P | 0.6 |
| $h_1$ | 0.64 |
| $h_2$ | 0.25 |

**Figure 4.** Implantable spiral planar antenna [18]. (a) Top view. (b) Bottom view. (c) Side view.

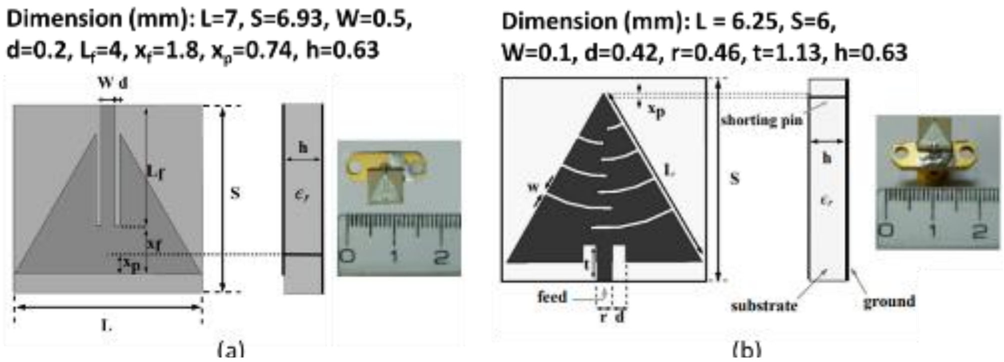


**Figure 5.** Meandered triangular microstrip antenna as an intraocular element [30]. (a) 2.45 GHz. (b) 1.45 GHz.

implantable antenna was recently proposed by the authors of [49]. The proposed antenna is comprised of a two-arm rectangular spiral microstrip resonator. This antenna size was 10 × 10 × 2.56 $mm^3$. The measured gain and bandwidth were, respectively, -18.41 dBi and 4.89% at 2.45 GHz.

### C. Fractal-geometry Antennas

Fractal geometry was defined by Mandelbrot in 1982 as "a set whose Hausdorff-Besicovitch dimension strictly exceeds its topological dimension [50]. Figure 6 presents various examples of fractal geometry. Designing an implantable antenna with fractal geometry reduces the dimension of the antenna. By using fractal geometry, one could extend the length of the electrical current path without the need to expand the antenna size. In this way, a smaller antenna could act as a larger radiator. Considering the space constraint of human tissue, obviously, miniaturization techniques are critical in implantable antenna design. In [19], the authors proposed a meander structure antenna with slot and fractal geometry. This proposed antenna operates at 2.45 GHz and was fabricated on a silicon substrate ($\epsilon_r = 11.7$). The dimensions of the proposed antenna were 11.44 × 11.44 × 0.275. This antenna has a measured bandwidth of 1.5%. In [44], a Gosper curve fractal-based geometry PIFA implantable antenna was proposed (See Figure 7). Thanks to the combination of two miniaturization techniques (i.e., fractal-geometry and PIFA), although this antenna operates at a relatively lower frequency of 0.402 GHz, its dimensions were only $\pi \times 5^2 \times 0.762$. This antenna has a measured gain of -39.58 dBi and a measured bandwidth of 10.1%.

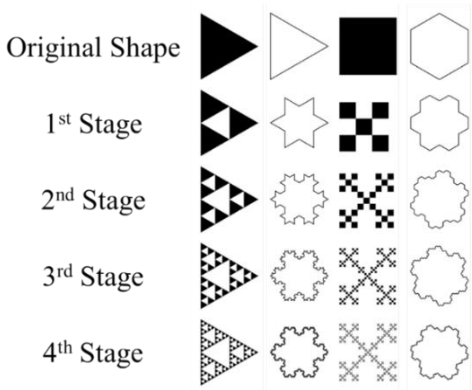


**Figure 6.** Various types of fractal-geometry.

### D. Conformal Antennas

Conformal antenna structure allows implantable antennas to be bent in a spherical manner, thus making it suitable for implantable wireless capsule systems without compromising the performance of the antennas. In [20], the authors proposed a conformal CP patch antenna that operated on 2.45 GHz. The dimensions of the antenna were 14.2 × 16.65 × 0.254 $mm^3$. This antenna was designed for wireless capsule endoscope system applications. The

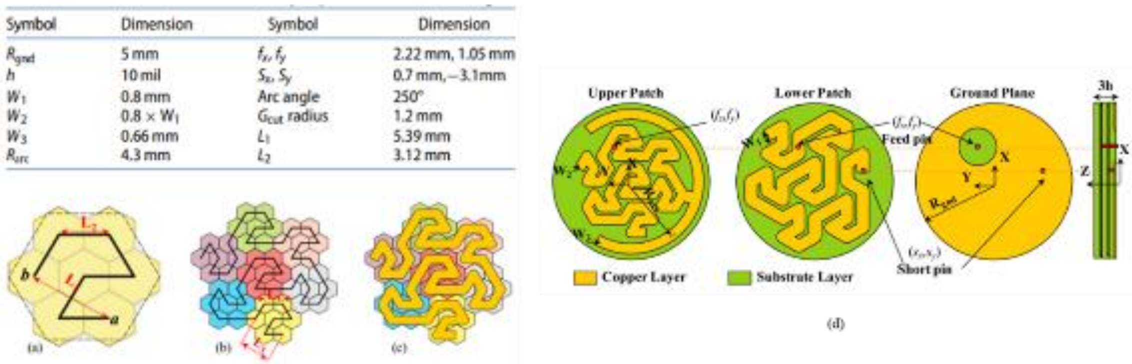


**Figure 7.** Proposed implantable antenna based on Gosper curve fractal geometry [44]. (a) First iteration. (b) Second iteration. (c) Antenna element design model. (d). Antenna geometry layout.

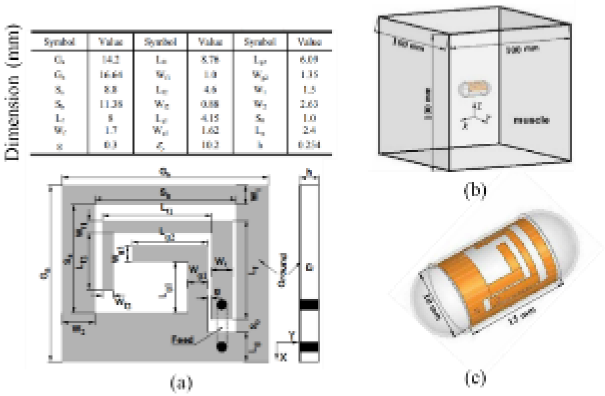


**Figure 8.** Design of the implantable conformal antenna proposed in [20]. (a). Planar view. (b) Muscle phantom. (c) Capsule antenna.

proposed antenna design is depicted in Figure 8. This antenna was manufactured on a Rogers RO6010 substrate and is capable of achieving -29.1 dBi peak gain and 31% bandwidth at 2.45 GHz. Another conformal antenna was proposed by the authors in [51]. However, this antenna was designed for both wireless monitoring and WPT. This antenna operated at 0.403 GHz, 1.5 GHz, and 2.4 GHz. By experiments, the authors showed that the proposed antenna is able to achieve up to 0.473% WPT efficiency at a 5.5 cm distance on a 1.5 GHz frequency.

## E. Spiral Antennas

In [48], a compact-sized multiband spiral-shaped implantable antenna was proposed. The antenna was designed for scalp implantable and leadless pacemaker systems. The proposed antenna worked on four different frequency bands: 0.402 MHz, 0.433 GHz, 1.6 GHz, and 2.45 GHz. As in Figure 9, in this work, the authors proposed an implantable antenna system consisting of a flat-type scalp implantable device and a capsule-type leadless pacemaker. The proposed antenna has a compact volume of 17.15 $mm^3$ (7 × 6.5 × 0.377 $mm^3$). The maximum realized gains were -30.5, -30, -22.6, and -18.2 dBi, respectively, at 0.402, 0.433, 1.6, and 2.45 GHz. When implanted in minced pork, the measured -10 dB bandwidths of the proposed antenna were 0.148 GHz (0.356–0.504 GHz), 0.173 GHz (1.520–1.693 GHz), and 0.213 GHz (2.316–2.529 GHz). These wide bandwidths cover different frequency band categories such as Medical Implant Communications Service (MICS) (0.402–0.405 GHz), Industrial, Scientific, and Medical (ISM) (0.4331–0.4348 GHz and 2.400–2.4835 GHz), and midfield (1.520–1.693 GHz). In [49], an implantable antenna with a spiral-shaped element was proposed for biosensing applications. The proposed antenna operated at 2.4-2.48 GHz. The dimensions of the proposed antenna were 10 × 10 × 2.56 $mm^3$. The proposed antenna has a directional radiation pattern with 3.18 dBi directivity. A 4.89% bandwidth and -18.41 dBi peak gain were measured using the proposed antenna.

## F. Slot Antennas

A 2.45 GHz dual-ring slot implantable antenna was proposed in [22]. In this work, the implantable antenna was fabricated in a flexible Kapton polyamide substrate. The dimensions of the antenna were 10 × 10 × 0.4 $mm^3$ (See Figure 10). The proposed antenna has a high gain of -9 dBi and a wide bandwidth of 57% at 2.45 GHz. A completely different shape of slot antenna was proposed in [37]. The authors designed a C-shaped slot that worked on two frequency bands (i.e., 0.915 GHz and 2.4 GHz). A controlled measurement showed that the proposed antenna achieved a peak gain of -28.9 dBi at 0.915 GHz and -29.5 dBi at 2.4 GHz. This antenna was fabricated on a Rogers RO3210 substrate.

## G. Planar Inverted-F Antenna (PIFA)

An implantable PIFA was proposed in [28]. PIFA is one of the antenna topologies that is commonly used to miniaturize an antenna. The proposed implantable antenna worked at 0.402 MHz Medical Device Radiocommunications Service (MedRadio) frequency band, with a -34.9 dBi measured peak gain and 52 MHz measured impedance bandwidth at a return loss of -10 dB. The antenna was evaluated using a minced pork medium. With a 1W delivered power, the maximum specific


p-ISSN: 2621-3761
e-ISSN: 2621-2889

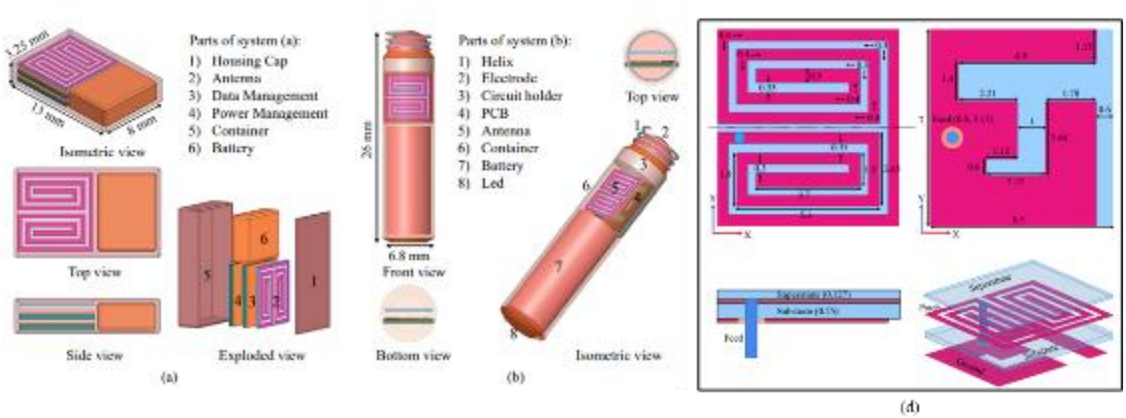


**Figure 9.** Multiband spiral-shaped implantable antenna proposed in [48]. (a) Scalp implantation device. (b) Leadless pacemaker. (c) The geometry of the antenna.

| L | S | W | $R_1$ | $R_2$ | h | D |
|---|---|---|---|---|---|---|
| 10 | 0.85 | 1 | 3.5 | 2.5 | 0.2 | 0.5 |

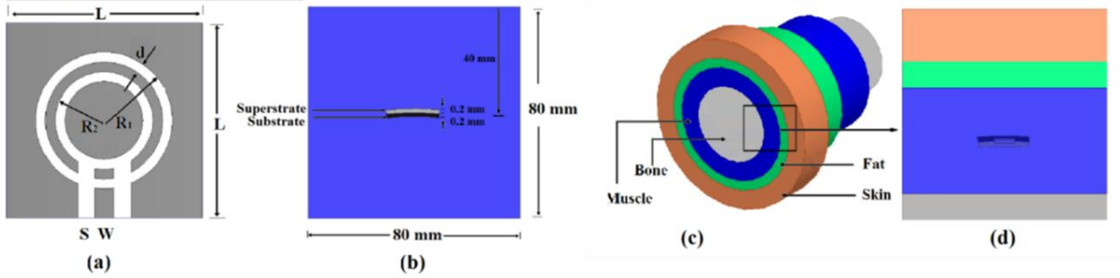


**Figure 10.** Geometry of implantable slot antenna in [22]. (a) Top view, (b) Antenna placed at the center of a cubic single layer human-muscle model. (c) 4-layer cylindrical human arm model. (d) Cross-section view of a cubic human arm model with the antenna implanted inside it.

absorption rate (SAR) value was 284.5 W/kg. A PIFA antenna was proposed as the extraocular element for the implanted and external subsystems of a wireless retinal prosthesis at 1.45 GHz in [30]. This antenna's dimensions were 28 × 24 × 1.43 mm$^3$. A dual-band PIFA implantable antenna was proposed in [36]. Figure 11 depicts the overall design of the proposed antenna. This antenna operated at 0.4025 MHz and 2.45 GHz. The antenna was sized at 19 × 27 × 0.635 mm$^3$. Similar to the antenna in [28] and [30], the proposed antenna in [36] was fabricated on a RO6010 substrate. This antenna achieves a slightly higher gain of -31 dBi at 0.402 MHz than those of [28] with -34.9 dBi.

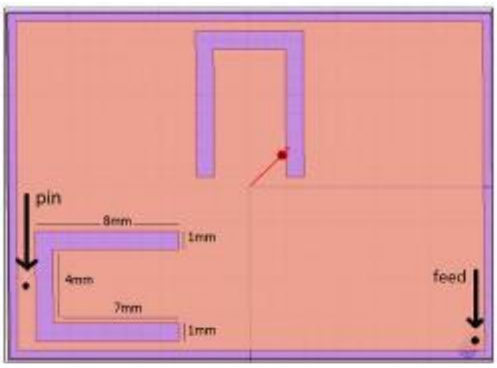


**Figure 11.** Design of the PIFA antenna proposed in [36].

## Material Selection

Antenna substrate is an important factor to consider in antenna design. An improper selection of antenna substrate may result in degraded performance. As summarized in Table 3, there are various substrates that have been used in implantable antenna design. In order to select the appropriate substrate, one must consider the characteristics of the substrate, mainly the dielectric constant and loss tangent. A substrate's dielectric constant depends on frequency and usually drops as the frequency rises. The degree of changes in dielectric constant varies between one substrate and another. In general, a substrate with stable dielectric constant over a broad range of frequencies is preferred for applications in high-frequency bands. As for the loss tangent, a substrate loses less power if its loss tangent is low. This property increases along with frequency. In Table 3, we summarize several types of substrates that are commonly used for implantable antenna applications. Rogers RO3000 series is commonly used due to its various advantages, such as high compatibility with multi-layers design, stable dielectric constant against frequencies and temperatures, low dielectric loss, and uniform mechanical properties. In conventional antenna and PCB design, FR-4 is arguably the most commonly used substrate. FR-4 is a cost-effective substrate that is compatible with a wide range of frequency bands.


p-ISSN: 2621-3761
e-ISSN: 2621-2889

However, although implantable antenna usually operates at 2.4 GHz frequency or lower, which is inside the FR-4 compatibility range, FR-4 is usually less preferred for this application, mainly due to its higher loss properties. Further, an implantable antenna that requires its structure to be flexible is typically fabricated using dielectric films, such as Kapton polyamide substrate, flexible biocompatible polyamide material, and liquid crystal polymer.

Different from the typical conventional antennas, in an implantable antenna design, several researchers proposed a combined superstrate-substrate structure. A superstrate layer is commonly used in implantable antenna design. A superstrate layer could prevent the conductor's contact with human tissue. In addition, a superstrate layer, such as Alumina ceramic ($Al_2O_3$), could increase the power penetration inside the human tissue as well as decrease SAR compared to the antenna without a superstrate [52]. Another approach to prevent conductor contact with human tissue is by encapsulating the implantable antenna with encapsulation materials. Polydimethylsiloxane (PDMS) material [53]–[55] is commonly used for encapsulating the antenna. In 2023, the authors [56] proposed a self-healing fluoroelastomer (SHFE) material for antenna encapsulation. In their study, the authors claimed that the SHFE exhibits a tissue-like modulus (approximately 0.4 MPa), stretchability (at least 450%, even after self-healing in an underwater environment), self-healability, and water resistance (WVTR result: 17.8610 g $m^{-2}$ $day^{-1}$), making SHFE a promising material for implantable antenna applications.

**Table 3.** Various Substrate/Superstrate Materials for Implantable Antennas

| **Substrate/Superstrate** | **Dielectric Constant/ Permittivity ($\epsilon_r$)** | **Loss Tangent (tan $\delta$)** |
|---|---|---|
| Rogers RO6010 | 10.2 | 0.0023 @ 10 GHz |
| Silicon substrate | 11.7 - 12.9 | 0.005 @ 1 GHz 0.015 @ 10 GHz |
| Kapton polyamide substrate | 3.9 (Type 100), 2.9 (Type 150) | |
| Rogers RO3010 | 10.02 | 0.0022 @ 10 GHz |
| Rogers ULTRALAM 3850HT | 3.14 | 0.002 @10 GHz |
| Duroid RT5880 | 2.2 | 0.0009 @ 10 GHz |
| Rogers RO3210 | 10.2 | 0.0027 @ 10 GHz |
| Rogers RO3003 | 3 | 0.001 @ 10 GHz |
| Flexible biocompatible polyamide material | 4.2 | 0.002 @ 2.45 GHz |
| Rogers RO4003 | 3.38 | 0.0027 at 10 GHz |
| Teflon, HIK500 | 11 | 0.002 |
| Zirconium dioxide (ZrO2) | 21 | 0.0013 |
| FR-4 | 4.2 (low resin), 4.9 (high resin) | 0.008 @ 100 MHz 0.008 @ 3 GHz |
| Alumina ceramic (Al2O3) 99.5% | 9.9 | 0.0001 |

## Available Frequency Bands for Biomedical Applications

In the area of implantable antennas for biomedical applications, the utilization of specific frequency bands is crucial to ensure reliable and efficient communication for various medical devices and systems. These frequency bands are allocated and regulated by international and national regulatory bodies to avoid interference and maintain the safety of patients and medical operations. In Table 4, we present various frequency bands designated for biomedical applications. The selection of frequency bands for implantable antennas for biomedical applications involves careful consideration of advantages and tradeoffs, especially between higher frequency bands and lower frequency bands. Each frequency range offers unique characteristics that can impact performance, efficiency, and safety in various medical devices and systems.

### A. Advantages of Higher Frequency Bands

- Increased Data Rate
  Higher frequency bands allow for higher data transmission rates, enabling rapid transfer of medical data. This is particularly advantageous for applications like medical imaging and real-time patient monitoring, where large amounts of data need to be transmitted quickly.
- Greater Bandwidth
  Higher frequency bands generally provide wider available bandwidth, allowing for the simultaneous transmission of multiple data streams. This is valuable for complex medical systems that require the coordination of multiple devices or data sources.
- Miniaturization of Antennas
  Antennas operating at higher frequencies can be physically smaller, making them suitable for miniaturized and implantable medical devices. This is especially important for devices like implants or wearable sensors where size constraints are critical.

### B. Tradeoffs of Higher Frequency Bands

- Propagation Loss and Attenuation
  Higher frequency signals are more susceptible to absorption and attenuation by human tissues. This can lead to reduced communication range and performance, especially for devices operating inside the body.
- Limited Penetration


p-ISSN: 2621-3761
e-ISSN: 2621-2889

**Table 4.** Frequency Bands Available for Biomedical Applications

| Category | Frequency Range (GHz) | Center Frequency (GHz) | Bandwidth (GHz) |
|---|---|---|---|
| **Industrial, Scientific, and Medical (ISM)**, defined by the International Telecommunication Union (ITU). | 0.43305 – 0.43479 | 0.43392 | $1.74 \times 10^{-3}$ |
| | 0.902 – 0.928 | 0.915 | $26 \times 10^{-3}$ |
| | 2.4 – 2.5 | 2.45 | $100 \times 10^{-3}$ |
| | 5.725 – 5.875 | 5.8 | $150 \times 10^{-3}$ |
| **Medical Device Radio Communications Service (MedRadio)**, defined by the U.S. Federal Communications Commission (FCC). | 0.401 – 0.406 | 0.4035 | $5 \times 10^{-3}$ |
| | 0.413 – 0.419 | 0.416 | $6 \times 10^{-3}$ |
| | 0.426 – 0.432 | 0.429 | $6 \times 10^{-3}$ |
| | 0.438 – 0.444 | 0.441 | $6 \times 10^{-3}$ |
| | 0.451 – 0.457 | 0.454 | $6 \times 10^{-3}$ |
| **Wireless Medical Telemetry Service (WMTS)**, defined by U.S. FCC. | 1.395 – 1.432 | 1.4135 | $37 \times 10^{-3}$ |
| **Medical Implant Communications Service (MICS)**, expanded to MedRadio, defined by U.S. FCC. | 0.402 – 0.405 | 0.4035 | $3 \times 10^{-3}$ |
| **Medical Body Area Networks (MBAN)**, defined by U.S. FCC. | 2.36 – 2.40 | 2.38 | $40 \times 10^{-3}$ |
| **Impulsive Radio Ultra-Wide Band (IR-UWB)**, defined by U.S. FCC. | 3-5 | 4 | 2 |
| **Wireless Body Area Network (WBAN) Ultra-Wide Band (UWB)**, defined by U.S. FCC. | 3.1 – 10.6 | 6.85 | 7.5 |
| **Medical Data Service Devices (MEDS)**, defined by the European Telecommunications Standards Institute (ETSI). | 0.401 – 0.402 | 0.4015 | $1 \times 10^{-3}$ |
| | 0.405 – 0.406 | 0.410 | $1 \times 10^{-3}$ |

Signals at higher frequencies have poorer penetration capabilities through obstacles, including the human body. This limits their suitability for applications requiring communication through walls or deep tissue layers.

- Increased Interference

  Higher frequency bands are more susceptible to interference from other electronic devices and environmental factors, potentially compromising the reliability of medical communication.

C. Advantages of Lower Frequency Bands

- Better Penetration

  Lower frequency signals exhibit improved penetration through obstacles, including the human body. This makes lower frequency bands well-suited for applications where communication needs to traverse walls or reach deep-seated devices.
- Reduced Absorption

  Lower frequency signals experience less absorption by biological tissues, resulting in improved communication range and efficiency for implanted devices.
- Lower Interference

  Lower frequency bands are often less crowded with competing signals, reducing the likelihood of interference from other electronic devices.

D. Tradeoffs of Lower Frequency Bands

- Limited Bandwidth

  Lower frequency bands typically offer narrower bandwidth, which can constrain data transmission rates and the capacity to support multiple devices simultaneously.
- Larger Antenna Size

  Antennas operating at lower frequencies tend to be larger in size, which can be a challenge for miniaturized medical devices or implants.
- Less Data Rate

  Lower frequency bands may not support as high data rates as higher frequency bands, which can be a limitation for applications requiring rapid data transfer.

## Implantable Rectifier Antenna (Rectenna)

The evolution of implantable antenna technology has spurred innovations in biomedical applications, and one noteworthy development in this realm is the concept of the implantable rectifier antenna, commonly referred to as a "rectenna." A rectenna integrates the functionality of an antenna and a rectifier into a single compact unit, enabling the wireless harvesting of energy from electromagnetic fields for implantable medical devices. The fundamental principle behind the Rectenna's design is to capture incident electromagnetic waves and convert their energy into usable direct current (DC) power through rectification. The typical structure of a rectenna is illustrated in Figure 12.

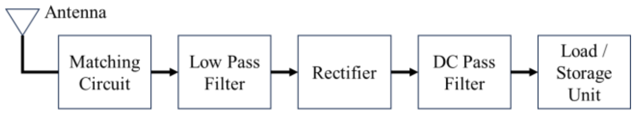


**Figure 12.** Overall structure of a typical rectenna.

The rectenna structure typically consists of an antenna element, a rectifying circuit, and an energy storage unit. The antenna element captures electromagnetic signals, such as those generated by external transmitters or ambient radiofrequency (RF) sources. These captured signals are then rectified by the integrated rectifying circuit, which converts the alternating current (AC) signal


p-ISSN: 2621-3761
e-ISSN: 2621-2889

**Table 5.** Recent Studies on Implantable Rectennas

| Ref. | Year | Topology | Frequency (GHz) | Dimension ($mm^3$) | Rectifier Components | WPT Total Distance (cm) | Measured WPT Efficiency (%) |
|---|---|---|---|---|---|---|---|
| [60] | 2019 | PIFA | 0.4035, 0.915 | 16 × 14 × 1.27 | Schottky Diode HSMS 2852 | n/a, 50 | n/a, up to 0.006 |
| [61] | 2022 | CP patch with four C-shaped open slots | 2.45 | 7.5 × 7.5 × 1.27 | Schottky Diode HSMS 2852 | 20 | Up to 0.00065 |
| [62] | 2020 | Compact patch antenna | 0.915 | $\pi \times 4^2 \times 1.27$ | Schottky Diode HSMS 2852 | n/a | n/a |
| [63] | 2020 | Meandering-line | 0.915, 1.9 | 5.6 × 6 × 0.2 | Schottky Diode HSMS 2860 | 2 | 0.25 at 0.915 GHz |
| [64] | 2019 | Circular-shaped radiating slot patch | 0.915 | 10.7 × 10.7 × 1.28 | Schottky Diode SMS 7630 | 18.5 | 0.213 |
| [65] | 2020 | Circular antenna | 0.402, 0.915 | $\pi \times 5.4^2 \times 1.28$ | Schottky Diode SMS 7630 | 150 | 0.0001 at 0.402 GHz |
| [66] | 2023 | Circular PIFA antenna | 0.915 | 8.382 × 11.176 × 1.5 | Schottky Diode HSMS 2862 | Up to 30 | n/a |
| [23] | 2018 | CP patch antenna | 0.910 | 11 × 11 × 1.27 | Schottky Diode HSMS 2850 | 2 | 0.01 |
| [67] | 2022 | Dual-band antenna based on a meandered-resonator | 0.915, 2.45 | 5 × 5.25 × 0.25 | Schottky Diode HSMS 2850 | 6 | 0.83, 1.3 |
| [68] | 2020 | Segment-cut circular meandered-line patch backed by a slotted ground | 0.403, 0.915, 1.47, 2.4 | 5 × 5 × 1.6 | Schottky Diode SMS 7630 | 5 | 0.67 at 1.47 GHz |
| [69] | 2019 | PIFA | 0.655 | $\pi \times 5^2 \times 1$ | Schottky Diode HSMS 285C | 50 | 0.06 |
| [51] | 2017 | Multiband conformal antenna | 0.403, 1.5, 2.4 | 20.5 × 31 × 1.6 | n/a | 5.5 | 0.473 at 1.5 GHz |
| [70] | 2023 | Patch antenna | 1.4 | 7 × 7 × 0.635 | Schottky Diode SMS 7630 | n/a | n/a |

into DC power suitable for powering or recharging implantable devices. The harvested energy can be stored in a supercapacitor or a rechargeable battery for later use by the medical device.

The integration of rectennas in implantable medical devices holds promise for addressing the challenge of powering and maintaining the functionality of such devices without the need for frequent battery replacements or invasive procedures. These devices range from sensors and stimulators to drug-delivery systems and neural implants. For instance, cardiac pacemakers and neurostimulators could benefit from rectenna technology by enabling longer device lifetimes and reducing the need for surgical interventions. Moreover, the rectenna's versatility extends to applications beyond power harvesting, including data communication. By modulating the reflected electromagnetic signal, the rectenna can also facilitate bidirectional communication between the implantable device and external systems.

While the rectenna presents an innovative solution for addressing power supply challenges in implantable devices, there are certain technical and safety considerations to address. Efficient energy harvesting requires careful tuning of the antenna and rectifier components to match the frequency of the incoming electromagnetic field. Additionally, the size constraints of implantable devices call for miniaturized rectenna designs that do not compromise energy conversion efficiency. Moreover, issues related to electromagnetic exposure, tissue compatibility, and regulatory approvals must be thoroughly addressed to ensure patient safety and compliance. Other challenges that arise in implantable rectenna design are WPT distance and WPT efficiency. In this work, the WPT distance refers to the transmitter-to-receiver total distance, while WPT efficiency refers to the total point-to-point efficiency, which can be calculated as

$$\text{WPT Efficiency } = \frac{P_{Tx}}{P_{Rx}} \times 100. \quad (4)$$

As depicted in Figure 12, typically, a rectenna contains rectifier components to convert the AC signals to DC signals. The selection of rectifier components and rectifier circuits is also crucial in rectenna design as it significantly affects the system's efficiency. The RF-to-DC conversion efficiency ($\varphi$) of a rectenna circuit can be expressed as

$$\varphi = \frac{\text{Harvested DC Power}}{\text{Input RF Power to Rectifier}} = \frac{P_{DC}}{P_{Rx}} \times 100\%, \quad (5)$$

where the $P_{Rx}$ can be obtained using the Friis equation

$$\frac{P_{Rx}}{P_{Tx}} = \left(\frac{A_{Tx}A_{Rx}}{d^2\lambda^2}\right) = G_{Tx}G_{Rx}\left(\frac{\lambda}{4\pi d}\right)^2, \quad (6)$$

where $P_{Tx}$ represents the power applied to the transmitting antenna's terminal, $P_{Rx}$ is the received power at the receiver terminal. $A_{Tx}$ and $A_{Rx}$ denote the effective aperture area of the transmitting and receiving antennas correspondingly. The variable $d$ refers to the distance of transmission between the antennas, while $\lambda$ represents the


p-ISSN: 2621-3761
e-ISSN: 2621-2889

wavelength of the radio frequency. Additionally, $G_{Tx}$ and $G_{Rx}$ denote the gain of the transmitting and receiving antennas, respectively.

In Table 5, we gathered some recent studies on implantable rectennas. As observed, at the moment, the efficiency of novel electromagnetic (EM)-based WPT systems is still too low, and the WPT range (i.e., distance) is still too short to be considered mature and ready to be massively deployed. Regardless, currently, RF-based WPT system has been able to power various low-power electronic devices [57]–[59]. In Table 6, we present the power consumption of some daily IoT devices. Given the demand for low-power IoT devices that often necessitate only minimal energy requirements, the future of WPT for implantable biomedical devices appears promising. With the capacity to provide power levels well-suited to these small-scale applications, WPT systems hold substantial potential in the biomedical arena. As advancements continue to refine the efficiency and reliability of WPT technology, the prospect of seamlessly powering implantable medical devices becomes increasingly feasible, heralding a future where wireless energy transfer contributes significantly to enhanced patient care and medical innovation.

**Table 6.** Power Consumption of Various IoT Devices

| Source | Device Type | Power Consumption |
|---|---|---|
| [56] | Wearable device | 60 µW |
| [58] | Smartwatch | 31 mW |
| [58] | CO sensor | 1.5 mW |
| [58] | LED | 60 mW |
| [58] | Gas sensor | 5.12 mW |
| [58] | WiFi flash memory | 210 µW |
| [58] | Smoke detector | 55 µW |
| [58] | Surveillance camera | A few mW |

## Antenna Miniaturization Technique

Antenna miniaturization is a pivotal aspect of modern biomedical applications, where size constraints often dictate the feasibility of implantable and wearable medical devices. Various techniques have been employed to achieve compact antenna designs while maintaining desired performance characteristics. Ground plane engineering involves optimizing the shape and size of the conductive ground plane to enhance antenna efficiency and reduce its physical footprint. By strategically modifying the ground plane, such as introducing various types of slots [71], reduction in the ground plane [71], the use of irregular ground structures [72], and defected ground structures (DGSs) [73], the antenna's resonant properties can be fine-tuned, leading to more compact designs.

Utilizing substrates with high permittivity is another effective approach. By selecting materials with elevated dielectric constants, the overall wavelength within the substrate is reduced, enabling smaller antenna dimensions. PIFA topology [44], [28], [36], [60], [66], [69] is commonly adopted for miniaturization, with its compact structure and ability to integrate into the device's casing. Fractal-geometry topology [19], [44] introduces self-similarity at different scales, enhancing miniaturization potential while preserving performance.

One of the simplest yet effective techniques for antenna miniaturization involves leveraging higher frequency bands. This approach takes advantage of the inherent properties of higher frequencies to achieve compact antenna designs while maintaining or enhancing performance characteristics. Higher frequency bands inherently have shorter wavelengths, which allows for the reduction of antenna dimensions while preserving resonance and radiation efficiency. This miniaturization technique is particularly beneficial for applications where size constraints are critical, such as implantable medical devices or wearable sensors. By operating in higher frequency ranges, antennas can be designed with smaller radiating elements and reduced ground plane size, contributing to overall device miniaturization.

While higher frequency bands offer the advantage of smaller antenna dimensions, there are certain considerations to keep in mind. The shorter wavelength can lead to challenges related to signal propagation and penetration. Higher frequency signals are more susceptible to absorption by biological tissues, potentially limiting the communication range within the body. Additionally, the increased likelihood of interference from other electronic devices and environmental factors must be addressed when designing antennas for higher frequency bands.

Another miniaturization technique that can be used in implantable antennas is inductor-capacitor (LC) loading [74]. LC loading involves introducing reactive elements to the antenna's structure, effectively altering its electrical length to achieve resonance at a reduced physical size. Shorting techniques use strategically placed shorting pins or vias to create virtual electrical paths, enabling the antenna to fit within confined spaces. Additionally, introducing slots into the antenna's radiating element can reshape the current distribution and enhance miniaturization. Folding and multi-layer patch configurations cleverly manipulate the antenna's geometry, effectively reducing its physical extent while maintaining adequate radiation performance.

An emerging approach for antenna miniaturization involves incorporating metamaterials [75], [76]. These engineered materials exhibit unique electromagnetic properties, such as negative permittivity or permeability, enabling novel antenna designs with reduced size. Metamaterial-based antennas leverage subwavelength resonances and wave manipulation, enabling antennas to operate at significantly reduced dimensions compared to conventional designs. In conclusion, a combination of ground plane engineering, substrate choice, topology selection (e.g., PIFA, fractal), frequency-specific techniques (LC loading, shorting), and innovative approaches such as metamaterial integration, collectively empower antenna miniaturization for the evolving landscape of IMDs for biomedical applications.

**Table 7.** Antenna Miniaturization Techniques

| Miniaturization Technique | Advantages | Possible Tradeoff |
|---|---|---|
| Ground plane engineering | Simple technique without significant changes in the antenna geometry. | Possible electromagnetic compatibility problem. Lower efficiency. Increased back lobe level |
| Substrate with high permittivity | A very straightforward technique. | Relatively narrower bandwidth. More expensive production cost. Surface wave issues could lead to efficiency degradation. |
| PIFA topology | Enabling a compact-size antenna with low backward radiation. Within the same frequency band, an implantable antenna can be packed into smaller dimensions if designed with PIFA topology. | Might reduce the gain of the antenna as the currents flowing at adjacent arms could cancel each other's. |
| Fractal-geometry topology | Longer current path. Makes a physically small antenna an electrically large radiator. The fractal-geometry miniaturization technique allows the antenna to be packed into smaller sizes without the need to move to higher frequency bands. | Intercell interference. Self-cancellation. Phase shift issue. These three factors might reduce the antenna performance. |
| Higher frequency bands | Higher frequency naturally enables smaller antennas due to the shorter wavelength of higher frequency bands. Introduce the potential of higher data rates and wider bandwidths. | Higher attenuation and propagation loss. More prone to interference. Due to the nature of higher-frequency bands. |
| Inductive-capacitive loading | Miniaturize antennas while mitigating impedance mismatch and reducing frequency shift. | Might reduce the antenna gain |
| Shorting technique | Cost-effective technique with a moderate degree of miniaturization | The antenna geometry will become more complex. Lower gain and directivity of the antenna. |
| Slots introduction | Miniaturization technique that could introduce a wider bandwidth | More complex antenna geometry. This technique could affect the radiation characteristics. |
| Folding and multi-layer patches | High degree of miniaturization. Cost-effective technique. | Complex antenna geometry. It could reduce the antenna gain and directivity. |
| The use of metamaterials | Relatively high degree of miniaturization. | Complex antenna design. No standardized design. Improper design could lead to a severe reduction in antenna performance. |

In Table 7, we summarize some key antenna miniaturization techniques along with their advantages and disadvantages.

## Biocompatibility and User Safety Considerations

### A. Specific Absorption Rate (SAR)

SAR is a crucial parameter in the evaluation of implantable antennas for biomedical applications, particularly those intended for communication or energy transfer within the human body. SAR quantifies the rate at which electromagnetic energy is absorbed by body tissues when exposed to electromagnetic fields. In the context of implantable antennas, understanding and managing SAR is paramount to ensure user safety, minimize tissue heating, and comply with regulatory standards. Table 8 presents the maximum allowed SAR and input power for various body parts according to FCC [42].

For implantable antennas, SAR assessment involves evaluating the potential for localized temperature elevation within tissues due to absorbed electromagnetic energy. Excessive SAR levels can lead to thermal damage to tissues or alter physiological processes, thereby posing significant risks to the user's health. Therefore, designers of implantable antennas must conduct rigorous simulations and experiments to accurately predict and measure SAR levels. These evaluations aid in identifying potential hotspots of energy absorption and enable adjustments in antenna design to mitigate elevated SAR values. Regulatory bodies, such as the International Commission on Non-Ionizing Radiation Protection (ICNIRP) and the U.S. FCC, have established SAR limits to safeguard users from adverse effects, reinforcing the importance of thorough SAR assessment in implantable antenna development. Table 10 encompasses various established SAR standards.

In general, any implantable RF system must adhere to the SAR standard. SAR refers to the time rate of change of incremental power that is either absorbed or dissipated within a defined volume of known density by an incremental mass [77]. The calculation of the SAR value is achievable through the following formula [78]

$$SAR = \frac{d}{dt}\left(\frac{dW}{dm}\right) = \frac{d}{dt}\left(\frac{dW}{\rho dV}\right). \quad (7)$$

Regarding the electric fields present at a specific location (such as within a human body or tissue), (7) can be restated as

$$SAR = \frac{\sigma}{\rho} \times E^2 \left[\frac{W}{kg}\right]. \quad (8)$$


p-ISSN: 2621-3761
e-ISSN: 2621-2889

Here, σ represents tissue conductivity [S/m], ρ signifies tissue mass density [kg/m3], and E denotes the root mean square (RMS) electric field strength [V/m].

In Table 9, we present some recent studies on implantable antennas with SAR evaluations. When designing implantable antennas, considerations must extend beyond traditional electromagnetic performance metrics and encompass SAR as a critical safety factor. Careful antenna geometry optimization, frequency selection, material selection, encapsulation, and placement within the body can all influence SAR levels. Advanced antenna designs, such as those that steer radiation away from sensitive tissues or distribute energy more evenly, can help manage SAR and reduce potential risks. Ultimately, the integration of SAR analysis into implantable antenna design practices underscores the commitment to user safety, ensuring that the benefits of wireless medical technology are realized without compromising the well-being of users.

**Table 8.** Max. Allowed SAR and Input Power (FCC) [42]

| Human Tissue | Max. SAR (W/Kg) | | Max. Input Power (mW) | |
|---|---|---|---|---|
| | **1 g** | **10 g** | **1 g** | **10 g** |
| Muscle | 712.2 | 78.86 | 2.8 | 20.28 |
| Kidney | 771.4 | 82.98 | 2.59 | 19.28 |
| Liver | 758.2 | 83.4 | 2.64 | 19.18 |
| Brain | 788.7 | 85.24 | 2.535 | 18.77 |
| Skin | 715.7 | 77.6 | 2.79 | 20.6 |
| Muscle | 712.2 | 78.86 | 2.8 | 20.28 |

**Table 9.** Recent Studies on Implantable Antennas with SAR Evaluations

| Ref. | Year | Frequency (GHz) | SAR (W/kg) | |
|---|---|---|---|---|
| | | | **1-g** | **10-g** |
| [16] | 2018 | 0.915<br>2.450 | 971<br>807 | 118<br>102 |
| [48] | 2018 | 0.402<br>1.600<br>2.450 | 588<br>441<br>305 | 92.7<br>85.3<br>81.7 |
| [46] | 2023 | 0.4025<br>2.45<br>2.95 | 189.42<br>124.246<br>145.094 | 42.0014<br>41.7769<br>39.572 |
| [42] | 2023 | 2.45 | 788.7 (Brain)<br>712.2 (Muscle)<br>715.7 (Skin)<br>758.2 (Liver)<br>771.39 (Kidney | n/a |
| [79] | 2021 | 0.91 | 481.1 (Intestine)<br>449.9 (Head) | n/a |
| | | 2.45 | 365.3 (Intestine)<br>312.7 (Head) | |

## B. Effective Isotropic Radiated Power (EIRP)

EIRP denotes the quantified radiated power of an antenna within a particular orientation. This parameter is also referred to as Equivalent Isotropic Radiated Power. Essentially, EIRP signifies the power output achieved when a signal is focused into a more confined region through the antenna. EIRP can be calculated as

$$\mathrm{EIRP} = \mathrm{P_{Tx}} - \mathrm{L_c} + \mathrm{G_A}, \tag{9}$$

where $\mathrm{P_{Tx}}$ is the transmit power (dBm), $\mathrm{L_c}$ is the cable loss (dB), and $\mathrm{G_A}$ (dBi) denotes the antenna gain. According to FCC, the maximum EIRP is 36 dBm (4 watt), whereas the maximum output power fed into the antenna is 30 dBm (1 watt).

## C. Maximum Permissible Exposure (MPE) Limit

The MPE is regulated to ensure that the radiation exposure toward the human body does not exceed the maximum safe limit. The MPE value depends on the frequency bands, and each governing body might have different standards. In 2.4 GHz, for example, the FCC stated that the maximum permissible exposure is 10 W/m$^2$ [81]. The power flux density at the distance $\mathrm{d_{tx-rx}}$ is calculated as [82]

$$[\mathrm{W_f}]_{\mathrm{W/m^2}} = \frac{\mathrm{EIRP}}{4\times\pi\times\, \mathrm{d_{tx-rx}}} \leq 10\,\frac{\mathrm{W}}{\mathrm{m^2}}. \tag{10}$$

## D. Focalized Temperature Limit

The rise in temperature within bodily tissues can result from the absorption of power generated by an electromagnetic field. It is of utmost importance to ensure that the temperature of the tissue encompassing the implanted device does not exceed an increase of 1 to 2 degrees Celsius [82].

## Human Body Effects on Implantable Antenna

Implantable antennas play a crucial role in enabling effective communication between implantable medical devices and external systems. However, the presence of the human body introduces several significant challenges and effects that can impact the performance of these antennas. Understanding these effects is essential for designing implantable antennas that can maintain reliable and efficient communication within the complex environment of the human body. Different than the materials mentioned in Table 3, human body parts are very lossy medium with diverse electrical properties (e.g., depending on the thickness, frequency, location, etc.). In Table 11, we gathered the electrical properties, such as the permittivity and electrical conductivity of various human body parts in 0.403 GHz, 0.915 GHz, and 2.45 GHz bands.


p-ISSN: 2621-3761
e-ISSN: 2621-2889

**Table 10.** Maximum Allowed SAR Standard According to Various Bodies

| Standard | | U.S. [80] | KR | JP [80] | CENELEC [80] | ICNIRP [80] | IEEE [80] |
|---|---|---|---|---|---|---|---|
| Frequency range (Hz) | | $10^5$ ~ $6\times10^8$ | $10^5$ ~ $10^{10}$ | $10^5$ ~ $3\times10^8$ | $10^4$ ~ $10^{11}$ | $10^5$ ~ $10^{10}$ | $10^5$ ~ $3\times10^9$ |
| Normal use (W/kg) | Whole body | 0.08 | 0.08 | 0.08 | 0.08 | 0.08 | 0.08 |
| | Head/ trunk | 1.6 | 1.6 | 2 | 2 | 2 | 2 |
| | Limbs | 4 | 4 | 4 | 4 | 4 | 4 |
| Occupational user (W/kg) | Whole body | 0.4 | 0.4 | 0.4 | 0.4 | 0.4 | 0.4 |
| | Head/ trunk | 8 | 8 | 10 | 10 | 10 | 10 |
| | Limbs | 20 | 20 | 20 | 20 | 20 | 20 |

*The limbs standard is derived from the average measurement for 10 grams of arbitrary human tissue. The term "Head/trunk" pertains to body regions other than the limbs. In the United States of America and Korea, the SAR standard for the head/trunk region is the highest average value for 1 gram of arbitrary human tissue. Conversely, Japan, CENELEC, ICNIRP, and IEEE standards adhere to an average value derived from 10 grams of generalized human tissue for the head/trunk category.

**U.S.:** United States of America
**KR:** Korea
**JP:** Japan
**CENELEC:** European Committee for Electrotechnical Standardization
**ICNIRP:** International Commission on Non-Ionizing Radiation Protection
**IEEE:** Institute of Electrical and Electronics Engineers

The attenuation loss inside the human body can be estimated as [14], [83]

$$L_\alpha = 20\log_{10}(e^{-\alpha L}). \quad (11)$$

where L(m) denotes the propagation distance inside the human body. The α(Np/m) denotes the attenuation constant, expressed as [14]

$$\alpha = \omega\sqrt{\frac{\mu\epsilon_r}{2}}\left(1+\left(\frac{\tau}{\omega\epsilon_r}\right)^2-1\right). \quad (12)$$

In addition to the attenuation loss inside the human body, the losses due to reflections at the boundary between body parts are estimated as [14]

$$L_r = 20\log_{10}(\Gamma). \quad (13)$$

### A. Human Body Effects on Radiation Efficiency

The human body is a complex medium that can significantly influence the radiation efficiency of implantable antennas. When an antenna is placed inside the body, the surrounding tissues can absorb and scatter electromagnetic waves. This absorption leads to losses and reduced radiation efficiency [1]. The dielectric properties of different tissues and their varying compositions introduce variations in how much energy is absorbed or radiated, affecting the overall efficiency of the antenna. Engineers must carefully consider these effects to ensure that the antenna's radiation efficiency remains within acceptable limits for reliable communication.

### B. Human Body Effects on Antenna Bandwidth

The presence of the human body can alter the antenna's resonant frequency and impedance matching due to the varying dielectric properties of different tissues. This can result in a shift in the antenna's bandwidth, affecting its ability to cover the desired frequency range. In addition, inside the human body, the absorbed power is usually much more than the reflected power, thus widening the bandwidth at the cost of lower radiation efficiency [1].

### C. Human Body Effects on Radiation Pattern

The radiation pattern of an implantable antenna defines how energy is radiated in different directions. The human body's presence can distort the radiation pattern, causing reflections, refractions, and multipath effects due to interactions with surrounding tissues and organs [84], [85]. These distortions can lead to variations in signal strength and directionality, impacting the overall communication link quality.

### D. Human Body Effects on Power Transfer Efficiency

In implantable medical devices, power transfer efficiency is a critical factor. Energy is often wirelessly transferred to the device for charging or operation. The human body's conductive properties can alter the impedance matching between the antenna and the device's power receiver. As a result, power transfer efficiency can be affected, leading to less effective energy transfer. Design considerations such as antenna placement, tuning, and impedance matching become vital in maintaining high power transfer efficiency while accounting for the presence of the human body.

## Implantable Antenna Design and Evaluation Methods

In this subsection, we present various design and evaluation methods of implantable antennas, summarized in Table 12. We divided these methods into three categories: computer simulation, in vivo experiments, and in vitro experiments. As in Table 12,


p-ISSN: 2621-3761
e-ISSN: 2621-2889

various simulation tools have been used in implantable antenna design and evaluation. In this regard, each tool has its own features and characteristics. Thus, it is hard to determine which simulation tool has the best performance. Regardless, it is quite often that the results produced in computer simulations differ from the actual real-world measurement. Thus, it is ideal to conduct real-world experiments, in addition to computer simulations, to evaluate the performance of the antenna.

There are two methods to measure the characteristics of an implantable antenna. In vitro measurements refer to the experiments conducted in non-living objects, such as saline solution, minced pork, and human phantom. In Figure 13, we present various examples of implantable antenna in vitro testing conducted by previous studies.

In vivo experiments refer to the measurement conducted in a living organism, such as a person, plant, or animal. Since the testing subject is alive, in vivo measurement arguably is the evaluation method that could produce results with better accuracy. However, this evaluation technique is also the most complicated one since we have to recruit a living organism, and we have to make sure that the test we conduct is ethical and will not introduce any harm to the test participants. In [87], the authors conducted an experiment by implanting an antenna into the chest of a pig. In [88], laboratory rats were recruited to test their proposed implantable intracranial antennas. A case report in [91] reported that a patient suffered an infection after they implanted an RFID into their hand. This has supported the importance of ensuring that implantable devices are safe and biocompatible before being implanted into a living being. In [92], an Asian volunteered themselves to receive an implantable antenna into their molar. Figure 14 depicts these in vivo measurement scenarios.

**Table 11.** Electrical Properties of Human Body Parts [86]

| Human Body Part | Permittivity ($\epsilon_r$) | | | Electrical Conductivity ($\tau$) (S/m) | | |
|---|---|---|---|---|---|---|
| | **0.403 GHz** | **0.915 GHz** | **2.45 GHz** | **0.403 GHz** | **0.915 GHz** | **2.45 GHz** |
| Bone (Cortical) | 13.1 | 12.4 | 11.4 | 0.0916 | 0.1450 | 0.3940 |
| Brain | 55.9 | 49.3 | 44.8 | 1.0300 | 1.2700 | 2.1000 |
| Cartilage | 45.4 | 42.6 | 38.8 | 0.5870 | 0.7890 | 1.7600 |
| Eye (Retina) | 57.4 | 52.7 | 48.9 | 0.7390 | 0.9490 | 1.8100 |
| Fat | 11.6 | 11.3 | 10.8 | 0.0808 | 0.1100 | 0.2680 |
| Heart Muscle | 66.0 | 59.8 | 54.8 | 0.9660 | 1.2400 | 2.2600 |
| Kidney | 66.3 | 58.6 | 52.7 | 1.1000 | 1.4000 | 2.4300 |
| Large Intestine | 62.5 | 57.9 | 53.9 | 0.8590 | 1.0900 | 2.0400 |
| Liver | 51.2 | 46.8 | 43.0 | 0.6550 | 0.8610 | 1.6900 |
| Muscle | 57.1 | 55.0 | 52.7 | 0.7970 | 0.9480 | 1.7400 |
| Skin | 46.7 | 41.3 | 38.0 | 0.6890 | 0.8720 | 1.4600 |
| Small Intestine | 66.1 | 59.4 | 54.4 | 1.9000 | 2.1700 | 3.1700 |
| Stomach | 67.5 | 65.0 | 62.2 | 1.0000 | 1.1900 | 2.2100 |
| Thyroid Gland | 61.5 | 59.7 | 57.2 | 0.8780 | 1.0400 | 1.9700 |
| Tooth | 13.1 | 12.4 | 11.4 | 0.0916 | 0.1450 | 0.3940 |

**Table 12.** Testing Methods for Implantable Antenna Evaluations

| Type of Evaluation Methods | Tools/Media | Study |
|---|---|---|
| Computer Simulations | FEKO | [91], [92] |
| | IE3D | [93], [94] |
| | CST | [42], [95] |
| | HFSS | [44], [96], [97], [98] |
| In Vitro Experiments | Pig Tissue (Minced, Raw Meat) | [79], [48], [89] |
| | Synthetic Human Skin | [89] |
| | Human Phantom | [48] |
| | Solution and Liquid (Water, Sugar, Salt, Saline) | [79], [99], [100] |
| | Dental Model/Animal Teeth | [90], [101] |
| In Vivo Experiments | Pig Tissue | [87] |
| | Rat Tissue | [88] |
| | Human Tissue/Bone | [102], [103] |

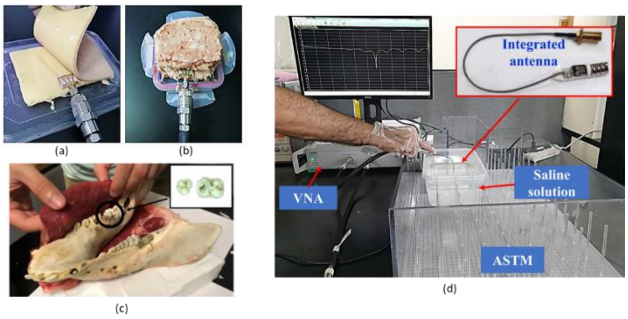


**Figure 13.** In vitro measurements. (a) Synthetic human skin [89]. (b) Minced pork [89]. (c) Porcine jaw [90]. (d) Saline solution [R7].

## IV. Conclusion

In this comprehensive review, we have undertaken an extensive examination of implantable antennas within the context of biomedical applications. The exploration of state-of-the-art advancements and associated challenges has shed light on the intricate interplay of design, performance, and safety considerations. Our analysis of antenna types, including planar, microstrip, fractal-geometry, and others, elucidated the nuances that govern


p-ISSN: 2621-3761
e-ISSN: 2621-2889

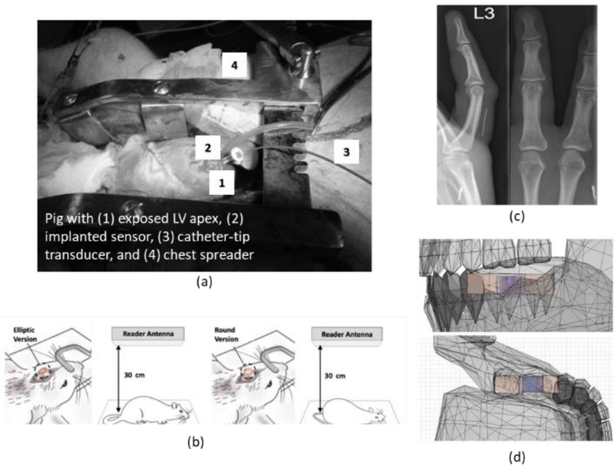


**Figure 14.** In vivo measurements. (a) Living pig [87]. (b) Laboratory rats [88]. (c) An X-ray of a human hand with two implanted RFIDs in it (One beside the middle finger bone and another beside the second metacarpal bone) [91]. (d) Lateral view and top view of teeth with an implanted antenna [92].

their suitability for diverse IMDs. The selection of substrates and materials emerged as a critical factor influencing antenna efficiency and biocompatibility. Our investigation into available frequency bands unveiled the tradeoffs inherent in their utilization for various biomedical purposes. The promising realm of rectenna technology was explored for its potential in sustainable energy harvesting. The discourse on miniaturization techniques underscored their pivotal role in accommodating antennas within intricate implant structures. Safety aspects took center stage, encompassing parameters such as SAR standards, EIRP limits, MPE limits, and focalized temperature thresholds. The complex interrelation between human body effects and antenna performance was a key focal point, unraveling insights that inform design strategies. Methodologies for evaluation, spanning computer simulations, as well as in vivo and in vitro experiment approaches, were scrutinized, emphasizing their importance in iteratively refining antenna functionality. As we conclude, we recognize the evolving landscape where engineering innovation, biomedical expertise, and regulatory guidelines converge to shape the trajectory of implantable antennas, guiding their integration into safer, more efficient, and transformative biomedical applications.

## Recommendations and Limitations

While this review offers a comprehensive analysis of implantable antennas for biomedical applications, certain limitations warrant consideration. The complexities surrounding the interaction of antennas with the human body, encompassing tissue heterogeneity and dynamic physiological changes, introduce variability that can impact antenna performance. Despite extensive investigation, a comprehensive understanding of the long-term biocompatibility and potential health implications of these antennas remains an ongoing challenge.

Furthermore, the evaluation of implantable antennas often relies on a combination of in vivo, in vitro, and simulation-based methodologies. However, achieving a harmonized framework that unifies these approaches while accounting for the dynamic and multifaceted nature of biological systems remains a notable endeavor.

In light of these limitations, future research endeavors could focus on refining antenna designs to mitigate the potential for tissue heating and electromagnetic interference. Exploring novel materials with improved biocompatibility profiles and enhanced electromagnetic characteristics could yield substantial advancements. Additionally, the integration of adaptive tuning mechanisms and impedance-matching techniques could enhance antenna resilience in complex physiological environments.

The investigation of alternative energy sources beyond traditional electromagnetic fields, such as harnessing physiological movements or biochemical processes, presents an intriguing avenue for sustainable implantable devices. Moreover, holistic studies that encompass the entire communication chain, including transmitter design and external device integration, would provide a more comprehensive understanding of the challenges and potential solutions.

## Acknowledgments

We would like to thank our colleagues in the Electrical Engineering Study Program of Universitas Ahmad Dahlan, Indonesia, and LPPM of Universitas Ahmad Dahlan, Indonesia, for their support for this study. This research was partially supported by the "*Penelitian Dosen Pemula Dana Internal*" Grant funded by LPPM of Universitas Ahmad Dahlan Indonesia (Grant No. PDP-271/SP3/LPPM-UAD/VIII/2023).

## References

[1] F. Merli, "Implantable antennas for biomedical applications," EPFL, 2011.

[2] C. Liu, Y.-X. Guo, and S. Xiao, "A review of implantable antennas for wireless biomedical devices," in *Forum for electromagnetic research methods and application technologies (FERMAT)*, 2016, pp. 1–11.

[3] M. M. Soliman *et al.*, "Review on medical implantable antenna technology and imminent research challenges," *Sensors*, vol. 21, no. 9, p. 3163, 2021.

[4] C. and T. European Commission Directorate-General for Communications Networks, "Smart Wearables: Reflection and Orientation Paper," Nov. 2016.

[5] U. K. Hisan, L. Y. Sabila, and M. M. Amri, "Coil-based Wireless Power Transfer for Implanted Pacemakers: A Brief Review," *Jurnal Teknik Elektro*, vol. 15, no. 1, pp. 1–7, 2023.

[6] E. M. McGee and G. Q. Maguire, "Becoming borg to become immortal: regulating brain implant technologies," *Cambridge Quarterly of Healthcare Ethics*, vol. 16, no. 3, pp. 291–302, 2007.

[7] J. Shin *et al.*, "Bioresorbable optical sensor systems for monitoring of intracranial pressure and temperature," *Sci Adv*, vol. 5, no. 7, p. eaaw1899, 2019.
[8] F.-G. Zeng, S. Rebscher, W. Harrison, X. Sun, and H. Feng, "Cochlear implants: system design, integration, and evaluation," *IEEE Rev Biomed Eng*, vol. 1, pp. 115–142, 2008.
[9] B. Mijnheer, "State of the art of in vivo dosimetry," *Radiat Prot Dosimetry*, vol. 131, no. 1, pp. 117–122, 2008.
[10] A. T. Chuang, C. E. Margo, and P. B. Greenberg, "Retinal implants: a systematic review," *British Journal of Ophthalmology*, vol. 98, no. 7, pp. 852–856, 2014.
[11] P. Rotter, B. Daskala, and R. Compano, "RFID implants: Opportunities and and challenges for identifying people," *IEEE Technology and Society Magazine*, vol. 27, no. 2, pp. 24–32, 2008.
[12] J. Lueke and W. A. Moussa, "MEMS-based power generation techniques for implantable biosensing applications," *Sensors*, vol. 11, no. 2, pp. 1433–1460, 2011.
[13] K. L. Baker, F. B. Bolger, and J. P. Lowry, "A microelectrochemical biosensor for real-time in vivo monitoring of brain extracellular choline," *Analyst*, vol. 140, no. 11, pp. 3738–3745, 2015.
[14] A. Kiourti and K. S. Nikita, "Miniature scalp-implantable antennas for telemetry in the MICS and ISM bands: Design, safety considerations and link budget analysis," *IEEE Trans Antennas Propag*, vol. 60, no. 8, pp. 3568–3575, 2012.
[15] R. Moore, "Effects of a surrounding conducting medium on antenna analysis," *IEEE Trans Antennas Propag*, vol. 11, no. 3, pp. 216–225, 1963.
[16] S. A. A. Shah and H. Yoo, "Scalp-implantable antenna systems for intracranial pressure monitoring," *IEEE Trans Antennas Propag*, vol. 66, no. 4, pp. 2170–2173, 2018.
[17] K. H. Yeap, E. M. F. Tan, T. Hiraguri, K. C. Lai, and K. Hirasawa, "A multi-band planar antenna for biomedical applications," *Frequenz*, vol. 75, no. 5–6, pp. 221–228, 2021.
[18] M. Ramzan, X. Fang, Q. Wang, N. Neumann, and D. Plettemeier, "Miniaturized planar implanted spiral antenna inside the heart muscle at MICS band for future leadless pacemakers," in *2019 13th International Symposium on Medical Information and Communication Technology (ISMICT)*, IEEE, 2019, pp. 1–4.
[19] S. Maity, K. R. Barman, and S. Bhattacharjee, "Silicon-based technology: Circularly polarized microstrip patch antenna at ISM band with miniature structure using fractal geometry for biomedical application," *Microw Opt Technol Lett*, vol. 60, no. 1, pp. 93–101, 2018.
[20] R. Li, Y.-X. Guo, and G. Du, "A conformal circularly polarized antenna for wireless capsule endoscope systems," *IEEE Trans Antennas Propag*, vol. 66, no. 4, pp. 2119–2124, 2018.
[21] Y. Zhang, C. Liu, X. Liu, K. Zhang, and X. Yang, "A wideband circularly polarized implantable antenna for 915 MHz ISM-band biotelemetry devices," *IEEE Antennas Wirel Propag Lett*, vol. 17, no. 8, pp. 1473–1477, 2018.
[22] S. Das and D. Mitra, "A compact wideband flexible implantable slot antenna design with enhanced gain," *IEEE Trans Antennas Propag*, vol. 66, no. 8, pp. 4309–4314, 2018.
[23] C. Liu, Y. Zhang, and X. Liu, "Circularly polarized implantable antenna for 915 MHz ISM-band far-field wireless power transmission," *IEEE Antennas Wirel Propag Lett*, vol. 17, no. 3, pp. 373–376, 2018.
[24] A. E. Mohamed, M. S. Sharawi, and A. Muqaibel, "Implanted dual-band circular antenna for biomedical applications," *Microw Opt Technol Lett*, vol. 60, no. 5, pp. 1125–1132, 2018.
[25] L.-J. Xu, Y. Bo, W.-J. Lu, L. Zhu, and C.-F. Guo, "Circularly polarized annular ring antenna with wide axial-ratio bandwidth for biomedical applications," *IEEE Access*, vol. 7, pp. 59999–60009, 2019.
[26] G. Samanta and D. Mitra, "Dual-band circular polarized flexible implantable antenna using reactive impedance substrate," *IEEE Trans Antennas Propag*, vol. 67, no. 6, pp. 4218–4223, 2019.
[27] F. Faisal and H. Yoo, "A miniaturized novel-shape dual-band antenna for implantable applications," *IEEE Trans Antennas Propag*, vol. 67, no. 2, pp. 774–783, 2018.
[28] R. Li, B. Li, G. Du, X. Sun, and H. Sun, "A compact broadband antenna with dual-resonance for implantable devices," *Micromachines (Basel)*, vol. 10, no. 1, p. 59, 2019.
[29] N. Ganeshwaran, J. K. Jeyaprakash, M. G. N. Alsath, and V. Sathyanarayanan, "Design of a dual-band circular implantable antenna for biomedical applications," *IEEE Antennas Wirel Propag Lett*, vol. 19, no. 1, pp. 119–123, 2019.
[30] S. Bahrami, G. Moloudian, S. R. Miri-Rostami, and T. Björninen, "Compact microstrip antennas with enhanced bandwidth for the implanted and external subsystems of a wireless retinal prosthesi," *IEEE Trans Antennas Propag*, vol. 69, no. 5, pp. 2969–2974, 2020.
[31] Y. Feng, Z. Li, L. Qi, W. Shen, and G. Li, "A compact and miniaturized implantable antenna for ISM band in wireless cardiac pacemaker system," *Sci Rep*, vol. 12, no. 1, p. 238, 2022.
[32] P. Mohanraj and P. R. Selvakumaran, "Compact wideband implantable antenna for biomedical applications," *Current Applied Physics*, vol. 43, pp. 50–56, 2022.
[33] G. Wang, X. Xuan, D. Jiang, K. Li, and W. Wang, "A miniaturized implantable antenna sensor for wireless capsule endoscopy system," *AEU-International Journal of Electronics and Communications*, vol. 143, p. 154022, 2022.
[34] S. S. Mosavinejad, P. Rezaei, and A. A. Khazaei, "A miniaturized and biocompatible dual-band implantable antenna for fully-passive wireless signal monitoring," *AEU-International Journal of Electronics and Communications*, vol. 154, p. 154303, 2022.
[35] Y. E. Yamac, M. Ciflik, and S. C. Basaran, "Miniaturized multiband implantable antenna designs for in-body compact medical devices," *International Journal of RF and Microwave Computer-Aided Engineering*, vol. 32, no. 11, p. e23335, 2022.
[36] M. Matthaiou, S. Koulouridis, and S. Kotsopoulos, "A novel dual-band implantable antenna for pancreas telemetry sensor applications," in *Telecom*, MDPI, 2022, pp. 1–16.
[37] Y. Fan, X. Liu, and C. Xu, "A Broad Dual-Band Implantable Antenna for RF Energy Harvesting and Data Transmitting," *Micromachines (Basel)*, vol. 13, no. 4, p. 563, 2022.
[38] S. Ahmad, B. Manzoor, S. Naseer, N. Santos-Valdivia, A. Ghaffar, and M. I. Abbasi, "X-shaped slotted patch biomedical implantable Antenna for wireless

communication networks," *Wirel Commun Mob Comput*, vol. 2022, pp. 1–11, 2022.
[39] N. Abbas, S. A. A. Shah, A. Basir, Z. Bashir, A. Akram, and H. Yoo, "Miniaturized antenna for high data rate implantable brain-machine interfaces," *IEEE Access*, vol. 10, pp. 66018–66027, 2022.
[40] D. Jing, H. Li, X. Ding, W. Shao, and S. Xiao, "Compact and Broadband Circularly Polarized Implantable Antenna for Wireless Implantable Medical Devices," *IEEE Antennas Wirel Propag Lett*, 2023.
[41] A. D. Butt, J. Khan, S. Ahmad, A. Ghaffar, A. J. Abdullah Al-Gburi, and M. Hussein, "Single-fed broadband CPW-fed circularly polarized implantable antenna for sensing medical applications," *PLoS One*, vol. 18, no. 4, p. e0280042, 2023.
[42] A. Z. A. Zaki *et al.*, "Design and Modeling of Ultra-Compact Wideband Implantable Antenna for Wireless ISM Band," *Bioengineering*, vol. 10, no. 2, p. 216, 2023.
[43] R. Kangeyan and M. Karthikeyan, "Miniaturized meander-line dual-band implantable antenna for biotelemetry applications," *ETRI Journal*, 2023.
[44] R. Kumar, S. Singh, and A. P. S. Chauhan, "Implantable antenna design based on gosper curve fractal geometry," *IETE J Res*, vol. 69, no. 6, pp. 3583–3593, 2023.
[45] N. Abbas, S. Ullah, Z. Bashir, A. Basir, and H. Yoo, "Design and Measurement of a Minuscule-Sized Implantable Antenna for Brain-Machine Interfaces," *IEEE Access*, 2023.
[46] S. Salama, D. Zyoud, and A. Abuelhaija, "A Compact-Size Multiple-Band Planar Inverted LC Implantable Antenna Used for Biomedical Applications," *Micromachines (Basel)*, vol. 14, no. 5, p. 1021, 2023.
[47] S. M. A. Shah, M. Zada, J. Nasir, O. Owais, A. Iqbal, and H. Yoo, "Miniaturized Four-Port MIMO Implantable Antenna for High-Data-Rate Wireless-Capsule-Endoscopy Applications," *IEEE Trans Antennas Propag*, vol. 71, no. 4, pp. 3123–3133, 2023.
[48] I. A. Shah, M. Zada, and H. Yoo, "Design and analysis of a compact-sized multiband spiral-shaped implantable antenna for scalp implantable and leadless pacemaker systems," *IEEE Trans Antennas Propag*, vol. 67, no. 6, pp. 4230–4234, 2019.
[49] M. H. B. Ucar and E. Uras, "A Compact Modified Two-Arm Rectangular Spiral Implantable Antenna Design for ISM Band Biosensing Applications," *Sensors*, vol. 23, no. 10, p. 4883, 2023.
[50] B. B. Mandelbrot and B. B. Mandelbrot, *The fractal geometry of nature*, vol. 1. WH freeman New York, 1982.
[51] R. Das and H. Yoo, "A multiband antenna associating wireless monitoring and nonleaky wireless power transfer system for biomedical implants," *IEEE Trans Microw Theory Tech*, vol. 65, no. 7, pp. 2485–2495, 2017.
[52] M. R. Robel, A. Ahmed, A. Alomainy, and W. S. T. Rowe, "Effect of A Superstrate on On-Head Matched Antennas for Biomedical Applications," *Electronics (Basel)*, vol. 9, no. 7, p. 1099, 2020.
[53] R. P. Khokle, K. P. Esselle, M. Heimlich, and D. Bokor, "Design of a miniaturized bone implantable antenna for a wireless implant monitoring device," 2017.
[54] A. W. Damaj, H. M. El Misilmani, and S. Abou Chahine, "Implantable antennas for biomedical applications: An overview on alternative antenna design methods and challenges," in *2018 International Conference on High Performance Computing & Simulation (HPCS)*, IEEE, 2018, pp. 31–37.
[55] M. L. Scarpello *et al.*, "Design of an implantable slot dipole conformal flexible antenna for biomedical applications," *IEEE Trans Antennas Propag*, vol. 59, no. 10, pp. 3556–3564, 2011.
[56] S. An *et al.*, "A Water-Resistant, Self-Healing Encapsulation Layer for a Stable, Implantable Wireless Antenna," *Polymers (Basel)*, vol. 15, no. 16, p. 3391, 2023.
[57] P. Woznowski *et al.*, "A multi-modal sensor infrastructure for healthcare in a residential environment," in *2015 IEEE International Conference on Communication Workshop (ICCW)*, IEEE, 2015, pp. 271–277.
[58] O. Georgiou, K. Mimis, D. Halls, W. H. Thompson, and D. Gibbins, "How many Wi-Fi APs does it take to light a lightbulb?," *IEEE Access*, vol. 4, pp. 3732–3746, 2016.
[59] S. Naderiparizi, A. N. Parks, Z. Kapetanovic, B. Ransford, and J. R. Smith, "WISPCam: A battery-free RFID camera," in *2015 IEEE International Conference on RFID (RFID)*, IEEE, 2015, pp. 166–173.
[60] S. Bakogianni and S. Koulouridis, "A dual-band implantable rectenna for wireless data and power support at sub-GHz region," *IEEE Trans Antennas Propag*, vol. 67, no. 11, pp. 6800–6810, 2019.
[61] C. Xu, Y. Fan, and X. Liu, "A Circularly Polarized Implantable Rectenna for Microwave Wireless Power Transfer," *Micromachines (Basel)*, vol. 13, no. 1, p. 121, 2022.
[62] C. Xu, X. Liu, and Z. Li, "Miniaturized implantable rectenna for far-field wireless power transfer," in *2020 9th Asia-Pacific Conference on Antennas and Propagation (APCAP)*, IEEE, 2020, pp. 1–2.
[63] S. A. A. Shah and H. Yoo, "Radiative near-field wireless power transfer to scalp-implantable biotelemetric device," *IEEE Trans Microw Theory Tech*, vol. 68, no. 7, pp. 2944–2953, 2020.
[64] S. Ding, S. Koulouridis, and L. Pichon, "Implantable rectenna system for biomedical wireless applications," in *2019 IEEE Wireless Power Transfer Conference (WPTC)*, IEEE, 2019, pp. 454–457.
[65] S. Ding, S. Koulouridis, and L. Pichon, "Implantable wireless transmission rectenna system for biomedical wireless applications," *IEEE Access*, vol. 8, pp. 195551–195558, 2020.
[66] U. C. Resende, J. L. Soares, S. T. M. Gonçalves, and I. V Soares, "Design of a Fully Printed Implantable Rectenna".
[67] A. Iqbal, P. R. Sura, M. Al-Hasan, I. Ben Mabrouk, and T. A. Denidni, "Wireless power transfer system for deep-implanted biomedical devices," *Sci Rep*, vol. 12, no. 1, p. 13689, 2022.
[68] A. Basir and H. Yoo, "Efficient wireless power transfer system with a miniaturized quad-band implantable antenna for deep-body multitasking implants," *IEEE Trans Microw Theory Tech*, vol. 68, no. 5, pp. 1943–1953, 2020.
[69] A. Abdi and H. Aliakbarian, "A miniaturized UHF-band rectenna for power transmission to deep-body implantable devices," *IEEE J Transl Eng Health Med*, vol. 7, pp. 1–11, 2019.
[70] J. Zhang *et al.*, "Highly Integrated and Ultra-Compact Rectenna with Wireless Powering for Implantable Vascular Devices," in *2023 21st IEEE Interregional NEWCAS Conference (NEWCAS)*, IEEE, 2023, pp. 1–5.
[71] M. U. Khan, M. S. Sharawi, and R. Mittra, "Microstrip patch antenna miniaturisation techniques: a review," *IET*

*Microwaves, Antennas & Propagation*, vol. 9, no. 9, pp. 913–922, 2015.
[72] D. Wang, H. Wong, and C. H. Chan, “Miniaturized circularly polarized patch antenna by substrate integrated irregular ground,” in *2011 IEEE International Symposium on Antennas and Propagation (APSURSI)*, IEEE, 2011, pp. 1875–1877.
[73] A. B. Mustafa and T. Rajendran, “An effective design of wearable antenna with double flexible substrates and defected ground structure for healthcare monitoring system,” *J Med Syst*, vol. 43, pp. 1–11, 2019.
[74] S. H. Kim and J. H. Jang, “Compact folded monopole antenna with LC-loadings,” in *2010 International Workshop on Antenna Technology (iWAT)*, IEEE, 2010, pp. 1–4.
[75] R. O. Ouedraogo, E. J. Rothwell, A. R. Diaz, K. Fuchi, and A. Temme, “Miniaturization of patch antennas using a metamaterial-inspired technique,” *IEEE Trans Antennas Propag*, vol. 60, no. 5, pp. 2175–2182, 2012.
[76] E. J. Rothwell and R. O. Ouedraogo, “Antenna miniaturization: definitions, concepts, and a review with emphasis on metamaterials,” *J Electromagn Waves Appl*, vol. 28, no. 17, pp. 2089–2123, 2014.
[77] D. Seabury, “An update on SAR standards and the basic requirements for SAR assessment,” *Feature Article, Conformity*, pp. 1–8, 2005.
[78] S. Kovar, I. Spano, G. Gatto, J. Valouch, and M. Adamek, “SAR evaluation of wireless antenna on implanted cardiac pacemaker,” *J Electromagn Waves Appl*, vol. 31, no. 6, pp. 627–635, 2017.
[79] M. Al-Hasan, P. R. Sura, A. Iqbal, J. J. Tiang, I. Ben Mabrouk, and M. Nedil, “Low-profile dual-band implantable antenna for compact implantable biomedical devices,” *AEU-International Journal of Electronics and Communications*, vol. 138, p. 153896, 2021.
[80] H. M. Madjar, “Human radio frequency exposure limits: An update of reference levels in Europe, USA, Canada, China, Japan and Korea,” in *2016 International symposium on electromagnetic compatibility-EMC EUROPE*, IEEE, 2016, pp. 467–473.
[81] R. A. Bercich, D. R. Duffy, and P. P. Irazoqui, “Far-field RF powering of implantable devices: Safety considerations,” *IEEE Trans Biomed Eng*, vol. 60, no. 8, pp. 2107–2112, 2013.
[82] C. Liu, Y.-X. Guo, H. Sun, and S. Xiao, “Design and safety considerations of an implantable rectenna for far-field wireless power transfer,” *IEEE Trans Antennas Propag*, vol. 62, no. 11, pp. 5798–5806, 2014.
[83] S. Gabriel, R. W. Lau, and C. Gabriel, “The dielectric properties of biological tissues: II. Measurements in the frequency range 10 Hz to 20 GHz,” *Phys Med Biol*, vol. 41, no. 11, p. 2251, 1996.
[84] Q. H. Abbasi, M. U. Rehman, K. Qaraqe, and A. Alomainy, *Advances in body-centric wireless communication: Applications and state-of-the-art*. Institution of Engineering and Technology, 2016.
[85] M. Ur-Rehman, Q. H. Abbasi, M. Akram, and C. Parini, “Design of band-notched ultra wideband antenna for indoor and wearable wireless communications,” *IET Microwaves, Antennas & Propagation*, vol. 9, no. 3, pp. 243–251, 2015.
[86] Foundation for Research on Information Technologies in Society (IT’IS), “Dielectric Properties of Human Tissues,” *https://itis.swiss/virtual-population/tissue-properties/database/dielectric-properties/*, 2023.
[87] O. H. Murphy *et al.*, “Continuous in vivo blood pressure measurements using a fully implantable wireless SAW sensor,” *Biomed Microdevices*, vol. 15, pp. 737–749, 2013.
[88] S. Ma, T. Björninen, L. Sydänheimo, M. H. Voutilainen, and L. Ukkonen, “Double split rings as extremely small and tuneable antennas for brain implantable wireless medical microsystems,” *IEEE Trans Antennas Propag*, vol. 69, no. 2, pp. 760–768, 2020.
[89] K. Yeap, C. Voon, T. Hiraguri, and H. Nisar, “A compact dual-band implantable antenna for medical telemetry,” *Microw Opt Technol Lett*, vol. 61, no. 9, pp. 2105–2109, 2019.
[90] N. Panunzio *et al.*, “Cyber-tooth: Antennified dental implant for RFID wireless temperature monitoring,” in *2021 IEEE International Conference on RFID Technology and Applications (RFID-TA)*, IEEE, 2021, pp. 211–214.
[91] J. Liska, M. Gao, L. Jelinek, E. R. Algarp, A. K. Skrivervik, and M. Capek, “Upper Bound on Implantable Antennas Considering Ohmic Loss,” *arXiv preprint arXiv:2307.16466*, 2023.
[92] J. Kim, “Compact implantable antenna integrated with a wireless power transfer coil,” in *2020 Antenna Measurement Techniques Association Symposium (AMTA)*, IEEE, 2020, pp. 1–4.
[93] S. A. Kumar and T. Shanmuganantham, “Scalp–Implantable Antenna for Biomedical Applications,” in *2020 URSI regional conference on radio science (URSI-RCRS)*, IEEE, 2020, pp. 1–4.
[94] S. Manna, T. Bose, and R. Bera, “Microstrip patch antenna with fractal structure for on-body wearable medical devices,” in *Biotechnology and Biological Sciences: Proceedings of the 3rd International Conference of Biotechnology and Biological Sciences (BIOSPECTRUM 2019), August 8-10, 2019, Kolkata, India*, CRC Press, 2019, p. 25.
[95] T. Sathiyapriya, V. Gurunathan, and J. Dhanasekar, “Design of an implantable antenna for biomedical applications,” 2021.
[96] S. Hout and J.-Y. Chung, “Design and characterization of a miniaturized implantable antenna in a seven-layer brain phantom,” *IEEE Access*, vol. 7, pp. 162062–162069, 2019.
[97] N. Saini, J. Pahuja, H. Yadav, S. Sharma, Y. S. Rawat, and R. K. Nehra, “Bandwidth Enhancement of Implantable Antenna using Sorting PIN and Slot for BMDs,” *Research and Applications: Emerging Technologies*, vol. 5, no. 2, pp. 1–6, 2023.
[98] S. Shekhawat, G. Gunaram, V. Sharma, and D. Bhatnagar, “CPW fed implantable elliptical patch antenna for biomedical application,” in *AIP Conference Proceedings*, AIP Publishing, 2020.
[99] R. Dubey, V. R. Gupta, and M. K. Meshram, “Implantable slot antenna for biomedical application,” *International Journal of Advances in Microwave Technology*, vol. 6, no. 3, pp. 264–268, 2021.
[100] M. Zada, I. A. Shah, A. Basir, and H. Yoo, “Ultra-compact implantable antenna with enhanced performance for leadless cardiac pacemaker system,” *IEEE Trans Antennas Propag*, vol. 69, no. 2, pp. 1152–1157, 2020.
[101] J. Xu, H. Sato, M. Motoyoshi, N. Suematsu, K. Yasui, and Q. Chen, “A low-loss and compact UHF RFID tag antenna for implanted denture,” *IEEE Journal of Radio Frequency Identification*, vol. 6, pp. 1–7, 2021.

[102] A. Schiffmann, M. Clauss, and P. Honigmann, "Biohackers and Self-Made Problems: Infection of an Implanted RFID/NFC Chip: A Case Report," *JBJS Case Connect*, vol. 10, no. 2, p. e0399, 2020.
[103] C.-L. Yang, C.-L. Tsai, and S.-H. Chen, "Implantable high-gain dental antennas for minimally invasive biomedical devices," *IEEE Trans Antennas Propag*, vol. 61, no. 5, pp. 2380–2387, 2013.

.

## Declarations

| | | |
|---|---|---|
| **Author contribution** | **:** | Muhammad Miftahul Amri was responsible for the entire research project. He also led the writing of the manuscript and the collaboration with the second author. Urfa Khairatun Hisan participated in the data collection, transcription and analysis. She also revised the manuscript. Dwi Sulisworo was responsible for the project supervision and manuscript revision. All authors approved the final manuscript. |
| **Funding statement** | **:** | This research was partially supported by the "Penelitian Dosen Pemula Dana Internal" Grant funded by LPPM of Universitas Ahmad Dahlan Indonesia (Grant No. PDP-271/SP3/LPPM-UAD/VIII/2023). |
| **Conflict of interest** | **:** | All authors declare that they have no competing interests. |
| **Additional information** | **:** | No additional information is available for this paper. |